5

Application of Artificial Neural Network for Mineral Potential Mapping

Saro Lee and Hyun-Joo Oh
Geoscience Information Center, Korea Institute of Geoscience and Mineral Resources (KIGAM), 92, Gwahang-no, Yuseong-gu, Daejeon 305-350 Republic of Korea

1. Introduction

Mineral exploration is a multidisciplinary task requiring the simultaneous consideration of numerous disparate geophysical, geological, and geochemical datasets (Knox-Robinson, 2000). The size and complexity of regional exploration data available to geologist are increasing rapidly from a variety of sources such as remote sensing, airbone geophysics, large commercially available geological and geochemical data (Brown et al., 2000). This demands more effective integration and analysis of regional and various of geospatial data with different formats and attributes. In addition, this needs spatial modeling techniques using observations regarding the association of mineral occurrences with various geological features in a qualitative manner.

Geographic Information System (GIS) methods are very useful for processing and combining data within maps in mineral potential mapping. The development of GIS-based methods for integration and analysis of regional exploration datasets has an important role in assisting the decision-making processes for geologists in selection of exploration area (Brown et al., 2000). More recently, the mineral exploration industry has taken this approach further and with the help of spatial data modeling in GIS (Partington, 2010).

The spatial modeling techniques been proposed for mineral potential mapping, such as weights of evidence model (Bonham-Carter et al., 1988, 1989; Agterberg et al., 1990; Xu et al., 1992; Rencz et al., 1994; Pan, 1996; Raines, 1999; Carranza & Hale, 2000; Tangestani & Moore, 2001; Carranza, 2004; Agterberg & Bonham-Carter, 2005; Jianping et al., 2005; Nykanen & Raines, 2006; Porwal et al., 2006; Roy et al., 2006; Nykänen & Ojala, 2007; Raines et al., 2007; Oh & Lee, 2008; Harris et al., 2008; Benomar et al., 2009), Bayesian network classifiers (Porwal et al., 2006), logistic regression (Chung and Agterberg, 1980; Agterberg, 1988; Oh & Lee, 2008), fuzzy logic (An et al., 1991; Bonham-Carter, 1994; Eddy et al., 1995; D'Ercole et al., 2000; Knox-Robinson, 2000; Luo & Dimitrakopoulos, 2003; De Quadros et al., 2006; Carranza et al., 2008; Nykänen, 2008), artificial neural networks (Singer & Kouda, 1996; Harris & Pan, 1999; Brown et al., 2000, 2003; Rigol-Sanchez et al., 2003; Behnia, 2007; Skabar, 2007; Oh & Lee, 2008), and an evidence theory model (Moon, 1990, 1993; An & Moon, 1993; Moon & So, 1995; Porwal et al., 2003; Carranza et al., 2005). Researches using GIS have involved comparison of methods (Harris et al., 2003; Oh & Lee, 2008) and resolutions of spatial data used for mapping mineral potential, development of advanced methods,

improvement of prediction accuracy, and case studies for mineral potential mapping. These approaches have been successfully applied to mineral resource appraisal.

Artificial neural network (ANN), one of the spatial modeling methods, has great potential in various fields of application such as pattern recognition, classification, identification, vision, speech, and control systems in solving complex problems. The artificial neural network has advantage compared with statistical methods. Firstly, the artificial neural network method is independent of the statistical distribution of the data and there is no need of specific statistical variables. Compared with the statistical methods, neural networks allow the target classes to be defined with much consideration to their distribution in the corresponding domain of each data source (Zhou, 1999). Mineral potential mapping is an example where ANN method can be applied because the deposit occurrence is usually controlled by numerous interlocking geological features with non-linear relationship. It is difficult to estimate a spatial recognition criteria for appropriate training data in processes of various geological factors to form the deposits on the surface (Nykanen, 2008). It is important to select the training data such as deposit- and non-deposit locations used as input to the ANN's learning algorithm, which is proposed that minimizes some targeted minimal error between the desired and actual outputs of the network (Paola & Schowengerdt, 1995, Skabar, 2005).

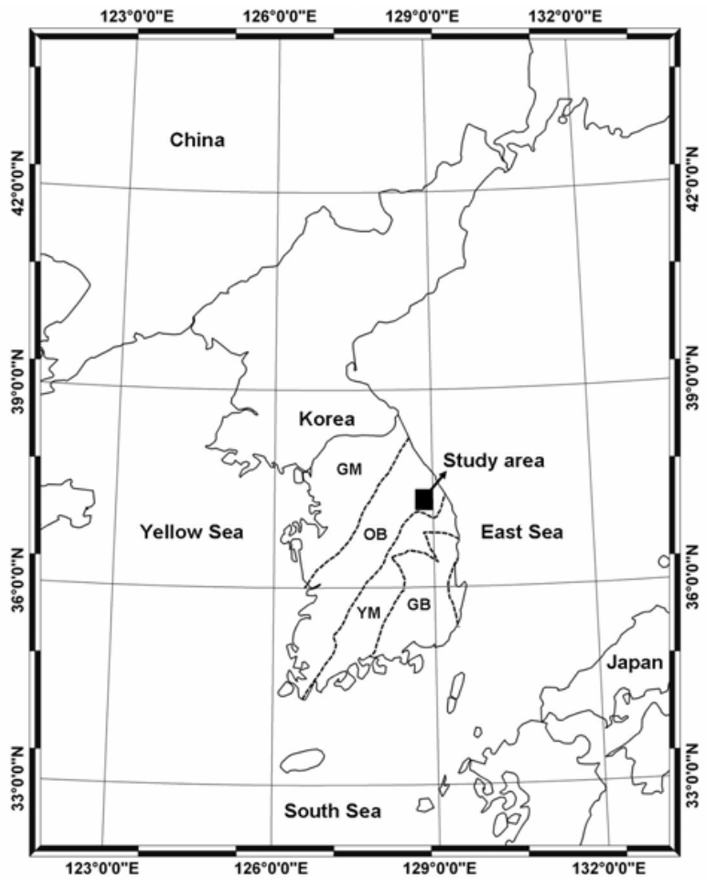

Fig. 1. Study area with tectonic units (GM = Gyeonggi Massif, OB = Ogcheon Belt, YM = Yeongnam Massif, GB = Gyeongsang Basin)

The objective of this study is to set some cases for selection of training data using quantitative mineral potential index by likelihood ratio, weights of evidence and logistic regression models, generate gold-silver potential maps using GIS and ANN to the various training sets, and estimate the predictive accuracy of those potential maps in the Taebaeksan mineralized district, Korea (Fig. 1). The preparation of mineral potential maps using GIS (ArcGIS 9.0) was accomplished in five major steps (Fig. 2): (1) Assembly of a spatial database. A total of 46 gold-silver mineral deposits were used to create a spatial database using GIS. Geological, geochemical and geophysical maps were similarly treated. (2) Processing the data from the database. The known mineral deposits were randomly split 70/ 30 for training/ testing, which used for analyzing and validating mineral potential maps using likelihood ratio, weights of evidence, logistic regression and ANN models (Leite & Souza Filho, 2009). Training locations (deposit and none-deposit occurrence) for ANN analysis were extracted from potential maps based on likelihood ration, weights of evidence and logistic regression models. Training dataset and the factors were analyzed and their weights were determined quantitatively. Especially, the nine cases for selection of training datasets determined from likelihood ratio, weights of evidence and logistic regression models were simulated to evaluate the sensitivity of ANN to training data. (3) Application of weights to generate a mineral potential map. (4) Validation of the potential map using test deposits that were not used directly in the analysis.

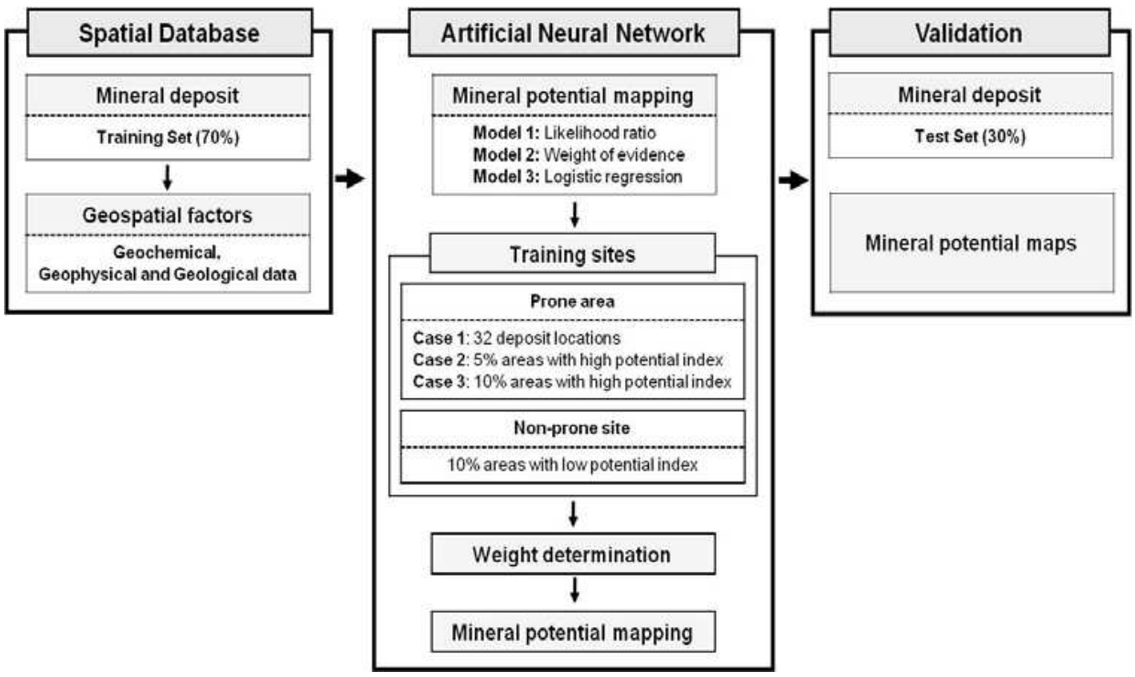

Fig. 2. Study flow for mineral potential mapping

2. Study area

The study area is bounded by latitudes 37°15´24´´–37°30´00´´ N and longitudes 128°30´30´´–129°02´40´´ E and lies in the Taebaeksan mineralized district at central east part of the

Korean Peninsula (Fig. 1). The total study area occupies approximately 1,050 km^2. The study area was chosen as high mineral potential area after regional gold-silver potential analysis in the Taebaeksan mineralized district (Oh & Lee, 2008). This region has many mineral deposits and geological, geochemical and geophysical survey data available.

Geological setting is largely distinguished by five groups of in the study area (Fig. 3). 1) Precambrian metamorphic and metasedimentary rocks (the unit Jugr and PCEt) in the northeastern part. 2) Cambro-Ordovician Joseon System (the unit CEj, CEm, CEp, CEw, Odu, Omg, Od and Oj) largely in the central part. 3) Carboniferous to Early Triassic Pyeongan System (the unit Ch, Ps, TRg, TRn3, TRn2, TRn1 and TRn) in the northwestern and southern parts. 4) Jurassic plutonic rocks (the unit Jigr) in the northern part and around the study area. 5) Cretaceous plutonic rocks (the unit Ksgr) in the southeastern part. Map-scale faults (~20km) trend mostly NNE-SSW and are of Late Cretaceous to Early Paleocene age (Fig. 3).

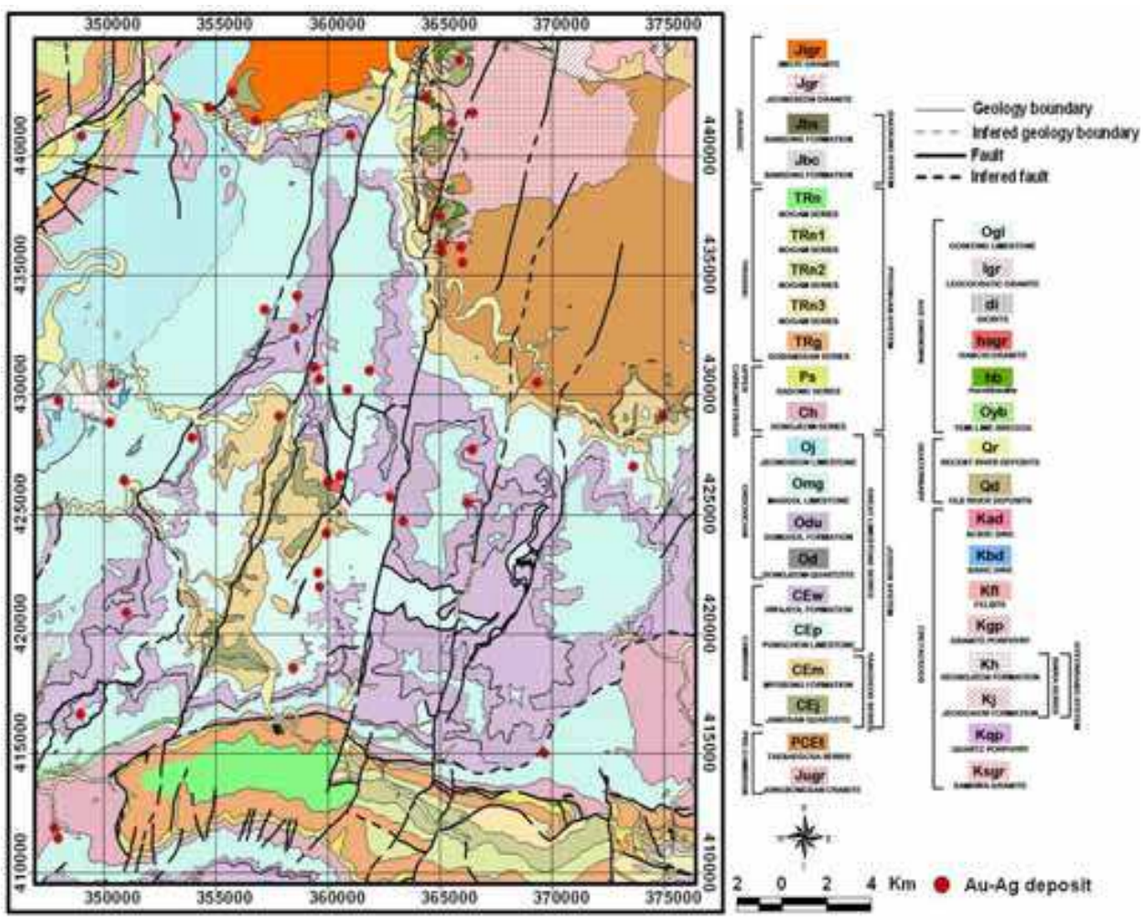

Fig. 3. Geological map with mineral deposits of the study area in Tabaeksan mineralized distract, Korea (combined geological map of Jeongseon, Imgye, Yemi and Homyeong sheets produced by the Korea Institute of Geoscience & Mineral Resources at 1:50,000)

Precambrian metamorphic rocks consist largely of banded gneiss, with lesser amounts of migmatitic gneiss, schist and quartzite. Additionally, there is abundant orthogenic granitic, garnet-bearing granitic, leucocratic and porphyroblastic gneiss incorporated within the complex unit. The Cambro-Ordovician Joseon System is mainly shallow marine in origin and consists predominantly of carbonates with lesser amounts of sandstone and shale, whereas the Carboniferous to Early Triassic Pyeongan System comprises thick clastic successions of marginal marine to non-marine environments. The Jurassic plutonic rock, Imgye Granite, mainly occurs as a large batholith trend NW-SE and as small stocks along the Ogcheon Belt consisting of granite with minor syenite and diorite. The Cretaceous plutonic rock, Samhwa Granite, mainly occurs as small stocks composed of granodiorite andesite, diorite, granite and granite porphyry (Kim et al., 1996, 2001).

Igneous rocks related to gold-silver deposits in the Korean Peninsula are Jurassic and Cretaceous granites. Gold-silver deposits are distributed in and around those granites. The Taebaeksan district is a famous metallogenic area that contains a variety of deposit types, including Cu-Fe-Au, W-Mo and Pb-Zn skarns, Pb-Zn-Ag hydrothermal carbonate replacement ores, Carlne-like, alakite, pegmatite, greisen and gold-silver vein deposits. Gold-silver bearing hydrothermal vein deposits in the study area occur in various host lithologies, consist of multiple generations of quartz and/ or carbonates with base metal sulphides, and have NNW, NS or NNE strikes, which seem to be related to NE strike-slip faults. Veins generally comprise quartz, lesser carbonate and polymetallic minerals including pyrite, sphalerite, galena, arsenopyrite, chalcopyrite and pyrrhotite. Electrum is the most common gold bearing ore mineral and the common silver-bearing phases are native silver, argentite, pyrargyrite and polybasite (Park et al., 1988; Lee & Park, 1996; Koh et al., 2003).

3. Spatial database

Data of hydrothermal gold-silver deposits were obtained from mineral deposit maps of the Taebaeksan mineralization with mineral variety and type, which were obtained from the MIRECO (Mine Reclamation Crop.), NHMRG (Natural Hazard Mitigation Research Group) and KIGAM (Korea Institute of Geoscience and Mineral Resources). The available factors related to gold-silver mineral occurrence are geophysical data of magnetic anomaly (Chi et al., 2001), geological data of geology and fault structure, and geochemical data of Al, As, Ba, Ca, Cd, Co, Cr, Cu, Fe, K, Li, Mg, Mn, Na, Ni, Pb, Si, Sr, V, W, Zn, Cl^- and F^- produced by KIGAM (Table 1). All of these factors were used within a spatial database with a pixel size of 30m x 30m. Most of the continuous data was classified into 10 equal-area classes. Categorical data, such as the geology, was set the unique attribute value to the each class. The numbers of rows and columns are, respectively, 986 and 1,183, and the total number of cells in the study area is 1,166,438. The number of mineral deposit occurrences is 46 and the number of factor is 26.

The geological data were derived from 1:50,000 geological maps (Jeongseon, Imgye, Yemi and Homyeong sheets). The geology and distance from fault were registered (Fig. 3). The geochemical maps were made from IDW (Inverse Distance Weighting) interpolation of values of geochemical elements, which were analyzed and collected from a stream water and sediment geochemical survey (Fig. A1a-w, Lee et al., 1998). The geophysical data was acquired through airborne magnetic surveys (Koo et al., 2001) (Fig. A1x).

Category	Factors	Data type	Scale	Remarks
Deposit	Au-Ag	Point	-	46 deposits
Geochemical Data	Al, As, Ba, Ca, Cd, Cl^-, Co, Cr, Cu, F^-, Fe, K, Li, Mg, Mn, Na, Ni, Pb, Si, Sr, V, W, Zn	Point	1:250,000	IDW (Inverse Distance Weight) Interpolation
Geological Data	Geology Distance from fault	Polygon Line	1:50,000	Combination of four geological map sheets
Geophysical Data	Magnetic anomaly	Point	1:250,000	IDW (Inverse Distance Weight) Interpolation

Table 1. Data layer of study area

4. Models

4.1 Artificial neural network model

An artificial neural network is a "computational mechanism able to acquire, represent, and compute a mapping from one multivariate space of information to another, given a set of data representing that mapping" (Garrett, 1994). The purpose of an artificial neural network is to build a model of the data-generating process, so that the network can generalize and predict outputs from inputs that it has not previously seen. The back-propagation is one of the most popular training algorithm used neural network method and is the method used in this study. The back-propagation algorithm trains network layer by layer doing forward and backward computation and is trained using a set of examples of associated input and output values. This learning algorithm is a multi-layered neural network, which consists of three layers; input, hidden and output. The hidden and output layer neurons process their inputs by multiplying each input by a corresponding weight, summing the product, then processing the sum using a log-sigmoid transfer function to produce a result (Fig. 4). An artificial neural network learns by adjusting the weights between the neurons in response to the errors between the actual output values and the target output values. At the end of this training phase, the neural network provides a model that should be able to predict a target value from a given input value (Lee et al., 2007).

There are two stages involved in using neural network for multi-source classification; the training stage, in which the internal weights are adjusted; and the classifying stage. Typically, the back-propagation algorithm trains the network until some targeted minimal error is achieved between the desired and actual output values of the network. Once the training is complete, the network is used as a feed-forward structure to produce a classification for the entire data (Paola & Schowengerdt, 1995).

A neural network consists of a number of interconnected nodes. Each node is a simple processing element that responds to the weighted inputs it received from other nodes. The arrangement of the nodes is referred to as the network architecture (Fig. 4). The receiving node sums the weighted signals from all nodes to which it is connected in the preceding layer. Formally, the input that a single node j receives is weighted according to Eq. (1):

$$net_j = \sum_i w_{ij} \cdot o_i \tag{1}$$

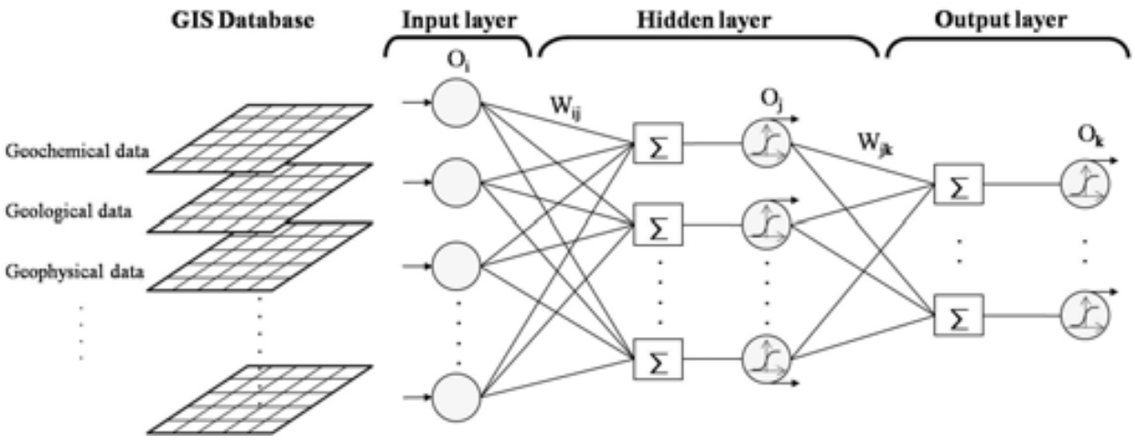

Fig. 4. The architecture of the artificial neural network

where w_{ij} represents the weight between node i and node j, and o_i is the output from node i such as Eq. (2):

$$o_j = f(net_j) \tag{2}$$

The valued produced by hidden node j, o_j, is the activation function, f, evaluated at the sum produced within node j, net_j, net_j, in turn, is a function of the weights between the input and hidden layer, w_{ij}, and the outputs of the input layer nodes, o_i. The function f is usually a non-linear sigmoid function that is applied to the weighted sum of inputs before the signal processes proceeds to the next layer. Advantage of the sigmoid function is that its derivative can be expressed in terms of the function itself such as Eq. (3):

$$f'(net_j) = f(net_j)(1 - f(net_j)) \tag{3}$$

The error, E, for one training pattern for input layer, t, is a function of the desired output vector, d, and the actual output vector, o, given by Eq. (4):

$$E = \frac{1}{2}\sum_k (d_k - o_k) \tag{4}$$

The error back propagated through neural network and the error is minimized by changing the weight between layers. So, the weight can be expressed by Eq. (5):

$$w_{ij}(n+1) = \eta(\delta_j \cdot o_i) + \alpha \Delta w_{ij} \tag{5}$$

where η is the learning rate parameter, δ_j is an index of the rate of change of the error, and α is the momentum parameter. This process of feeding forward signals and back propagating

the error is repeated iteratively until the error of the network as a whole is minimized or reaches an acceptable magnitude.

Using the backpropagation, the weight of each factor can be recognized and it can be used to weight determination for mineral potential. Zhou (1999) described the method of determination of the weight using backpropagation. From Eq. (2), the effect of an output o_j from a hidden layer node j on the output o_k from an output layer node k can be represented by the partial derivative of o_k with respect to o_j such as Eq. (6):

$$\frac{\partial o_k}{\partial o_j} = f'(net_k) \cdot \frac{\partial (net_k)}{\partial o_j} = f'(net_k) \cdot w_{jk} \tag{6}$$

The Eq. (6) equation can produce values with both positive and negative signs. If only the magnitude of the effects is of interest, the importance of node j relative to another node jo in the hidden layer can be calculated as the ratio of the absolute values from the Eq. (6):

$$\frac{\left|\partial o_k\right|}{\left|\partial o_j\right|} \Big/ \frac{\left|\partial o_k\right|}{\left|\partial o_{j0}\right|} = \frac{\left|f'(net_k) \cdot w_{jk}\right|}{\left|f'(net_k) \cdot w_{j0k}\right|} = \frac{\left|w_{jk}\right|}{\left|w_{j0k}\right|} \tag{7}$$

The Eq. (7) shows that, with respect to a particular node k in the output layer, the relative importance of a node j in the hidden layer is proportional to the absolute value of the weight on its connection to the node k in the output layer. When more than one node in the output layer is concerned, the Eq. (7) equation cannot be used to compare the importance of two nodes in the hidden layer. In other words, the relative importance of a node must somehow normalized to make it more comparable with that of other nodes. One choice is to let, in (7):

$$w_{j0k} = \frac{1}{J} \cdot \sum_{j=1}^{J} \left|w_{jk}\right| \tag{8}$$

to obtain the normalized importance of node j with respect to node k

$$t_{jk} = \frac{\left|w_{jk}\right|}{\frac{1}{J} \cdot \sum_{j=1}^{J} \left|w_{jk}\right|} = \frac{J \cdot \left|w_{jk}\right|}{\sum_{j=1}^{J} \left|w_{jk}\right|} \tag{9}$$

Therefore, with respect to the node k, each node in the hidden layer has a value greater or smaller than one, depending on whether it is more or less important than the average, respectively. With respect to the same node k, all the nodes in the hidden layer have a total importance such as Eq. (10):

$$\sum_{j=1}^{J} t_{jk} = J \tag{10}$$

Consequently, with respect to all nodes in the output layer, to which connected to hidden layer, the overall importance of node j can be calculated as Eq. (11):

$$t_j = \frac{1}{K} \cdot \sum_{k=1}^{K} t_{jk} \tag{11}$$

Similar to Eq. (9), with respect to the node j in the hidden layer, the normalized importance of the node i in the input layer can be defined as Eq. (12):

$$s_{ij} = \frac{\left|w_{ij}\right|}{\frac{1}{I} \cdot \sum_{i=1}^{I} \left|w_{ij}\right|} = \frac{I \cdot \left|w_{ij}\right|}{\sum_{i=1}^{I} \left|w_{ij}\right|} \tag{12}$$

With respect to the hidden layer, the overall importance of node i is done by Eq. (13):

$$s_i = \frac{1}{J} \cdot \sum_{j=1}^{J} s_{ij} \tag{13}$$

Correspondingly, the overall importance of the input node i with respect to the output node k is given by Eq. (14):

$$st_i = \frac{1}{J} \cdot \sum_{j=1}^{J} s_{ij} \cdot t_j \tag{14}$$

4.2 Likelihood ratio model

The likelihood ratio is a simple technique for producing a mineral potential map, and it is highly compatible with GIS. The likelihood ratio approach is based on observed relationships between the distribution of mineral deposits and each mineral deposit-related factor and are used to reveal the correlation between mineral deposit locations and factors in the study area. The likelihood ratio is the ratio of occurrence probability to non-occurrence probability for specific attributes.

For a given number of units cells, $N(D)$, containing a mineral deposit, D, and given number of total cells, $N(T)$, the prior probability of an occurrence is expressed by

$$P(D) = \frac{N(D)}{N(T)} \tag{15}$$

Now suppose that a binary predictor pattern, B, occupying $N(B)$ unit cells, occurs in the region, and that a number of known mineral deposits occur preferentially within the pattern, i.e., $N(D \cap B)$, then the probability of locating a deposit given the presence of a predictor(B), and the probability of a deposit occurrence in the absence of a pattern($\overline{B}$) can be expressed by the following conditional probabilities, respectively:

$$P(D \mid B) = \frac{P(D \cap B)}{P(B)} = P(D)\frac{P(B \mid D)}{P(B)} \tag{16}$$

$$P(D \mid \bar{B}) = \frac{P(D \cap \bar{B})}{P(\bar{B})} = P(D)\frac{P(\bar{B} \mid D)}{P(\bar{B})} \tag{17}$$

The posterior probability of a deposit occurrence given presence and absence of a favorable predictor pattern are denoted by $P(D \mid B)$ and $P(D \mid \bar{B})$, respectively. $P(B \mid D)$ and $P(\bar{B} \mid D)$ are the posterior probabilities of being inside and outside the predictor pattern B, respectively, given the presence of a deposit D. $P(B)$ and $P(\bar{B})$ are the prior probabilities of the presence of a predictor pattern B.

The odds, O, is defined as the ration of the probability P that an event will occur to the probability that the event will not occur; i.e. $O = P / \bar{P} = P(1-P)$. Expressed as odds, Eqs. 18 and 19 become:

$$O(D \mid B) = O(D)\frac{P(B \mid D)}{P(B \mid \bar{D})} \tag{18}$$

$$O(D \mid \bar{B}) = O(D)\frac{P(\bar{B} \mid D)}{P(\bar{B} \mid \bar{D})} \tag{19}$$

where $O(D \mid B)$ and $O(D \mid \bar{B})$ are the posterior odds of a deposit given the presence and absence of a binary predictor pattern B, respectively, and $O(D)$ is the prior odds of a deposit. The likelihood ratios, which are sufficiency ratio (LS) and necessity ratio (LN), are quire by the following equation:

$$LS = \frac{P(B \mid D)}{P(B \mid \bar{D})} \tag{20}$$

$$LN = \frac{P(\bar{B} \mid D)}{P(\bar{B} \mid \bar{D})} \tag{21}$$

To calculate the likelihood ratio for the class or type of each factor, all scale factors that consisted of a raster type were reclassified into 10 classes based on equal areas using GIS techniques. The cross tabulation in ArcGIS 9.0 was used to calculate the number of deposit occurrences in the class or type of each factor. The likelihood ratio was used to calculate the ratio of the cell with deposit occurrence in each class for a reclassified factor or categorical factor (i.e., geochemical data and geology), and the ratio was assigned to each factor class again. Finally, the likelihood ratios (Table A1) of each factor type or range were summed to calculate the Mineral Potential Index (MPI) (Fig. 5a), as shown in Eq. (22):

$$MPI_{LR} = Lr_1 + Lr_2 + Lr_3 + \ldots + Lr_n \tag{22}$$

where Lr_n = likelihood ratio of each factor type or range.

The MPI_{LR} represents relative potential of mineral deposit occurrence. The greater the value, the higher the potential of mineral deposit occurrence and the lower the value, the lower the

potential of mineral deposit occurrence. The mineral deposit potential map was made using the MPI_{LR} and was used for selecting training sites.

4.3 Weights of evidence model

The following application of Bayesian probability known as the likelihood ratio and weighs of evidence to mineral potential analysis was synthesized from Bonham-Carter (1994) and Bonham-Carter et al. (1989). A detailed description of the formulation of the weights of evidence method is available in Bonham-Carter et al. (1989) and Bonham-Carter (1994). The weights can be defined as shown in Eqs. 23 and 24:

$$W^{+} = \log_e LS \tag{23}$$

$$W^{-} = \log_e LR \tag{24}$$

$$C = W^{+} - W^{-} \tag{25}$$

$$S(c) = \sqrt{S^2(W^{+}) + S^2(W^{-})} \tag{26}$$

where W^{+} and W^{-} are the weights of evidence when a binary predictor pattern is present and absent, respectively and also shows the level of positive and negative correlation between the presence and absence of the predictable variable and the deposit occurrence. The difference between the W^{+} and W^{-} weight is known as the weight contrast, C. The C reflects the overall spatial association between the predictable variable and the mineral deposit. The $S^2(W^{+})$ and $S^2(W^{-})$ are variances of W^{+} and W^{-} and $S(C)$ is the standard deviation of the contrast. The studentized value of C, calculated as the ratio of C to its standard deviation, $C/S(C)$, serves as a guide to the significance of the spatial association, and becomes useful in determining cutoff value to convert multiclass evidential data into binary predictor maps (Bonham-Carter et al., 1989; Carranza, 2004). In this study the cutoff value within which their spatial association with a given pattern is most statistically significant was chosen based on the maximum studentized value of contrast(C/ s(C)).

To calculate the weights of evidence for the class or type of each factor, the same type of input factor as the likelihood ratio is used. The cell number of deposit occurrence in each class of reclassified or categorical factors was also calculated using cross tabulation function in ArcGIS. The binary predictor patterns were also assigned weights (Table A1) and were combined according to Eq. (27). The mineral potential map was shown in Fig. 5b.

$$MPI_{WOE} = Woe_1 + Woe_2 + Woe_3 + \ldots + Woe_n \tag{27}$$

where $Woe = W^{+}$ and W^{-} of the binary pattern for a range of each factor values or factor class.

The mineral deposit potential map was made using the MPI_{WOE} and was used for selecting training sites.

4.4 Logistic regression model

The logistic regression, which is one of the multivariate analysis models, is useful for predicting the presence or absence of a characteristic or outcome based on values of a set of spatial variables. The advantage of logistic regression is that, through the addition of an appropriate link a function to a usual linear regression model, the variables may be either continuous or discrete, or any combination of both types (Lee et al, 2007). In this study, the dependent variable is binary representing presence or absence of a mineral deposit and therefore a logistic link function is applicable (Atkinson & Massari 1998). For this study, the dependent variable must be input as either 0 or 1, so the method applies well to mineral potential analysis. Logistic regression coefficients can be used to estimate odds ratios for each of independent variables in the model. The relationship between the occurrence and its dependency on several variables can be expressed as:

$$p = 1/(1+e^{-z}) \tag{28}$$

where p is the probability of the event occurring and z is parameter. In this study, the p is the estimated probability of mineral deposit occurrence. The probability varies from 0 to 1 on an S-shaped curve and z is the linear combination. It follows that logistic regression involves fitting an equation of the following form to the data:

$$z = b_0 + b_1x_1 + b_2x_2 + \ldots + b_nx_n \tag{29}$$

where z is parameter, b_0 is the y-axis intercept, b_i ($i = 0, 1, 2, \ldots, n$) are the slope coefficients of the logistic regression model and the x_i ($i = 0, 1, 2, \ldots, n$) are the independent variables. The logistic regression coefficient values are listed in Table A1. The mineral potential map was made using Eqs. (28) and (29) and was used for selecting training sites.

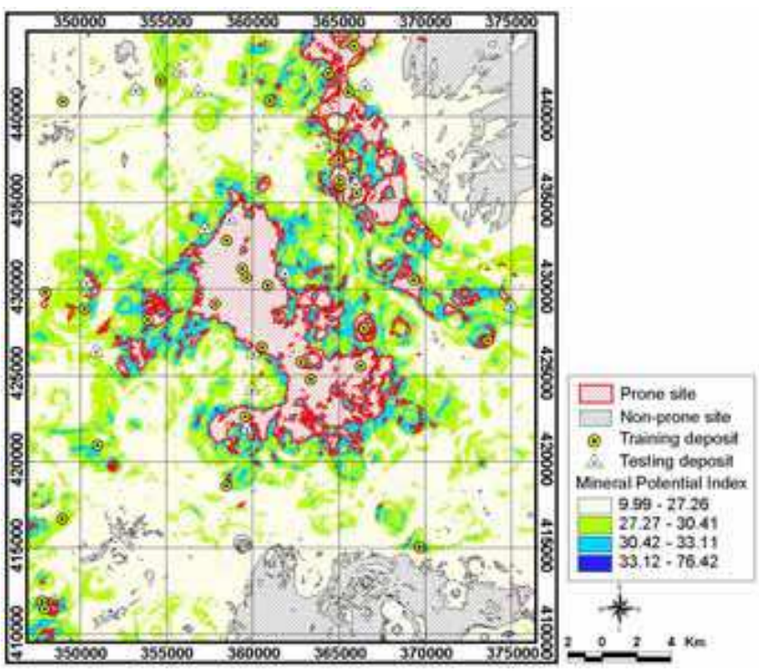

(a)

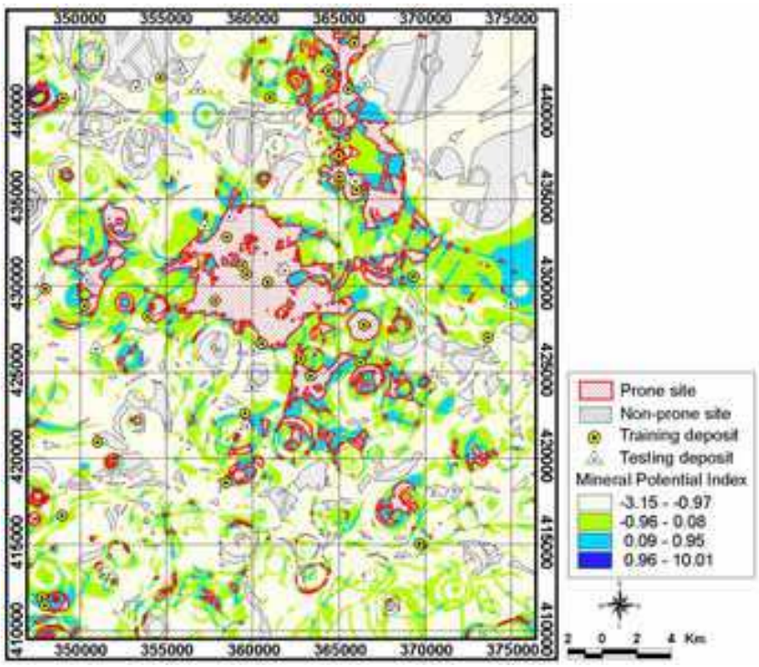

(b)

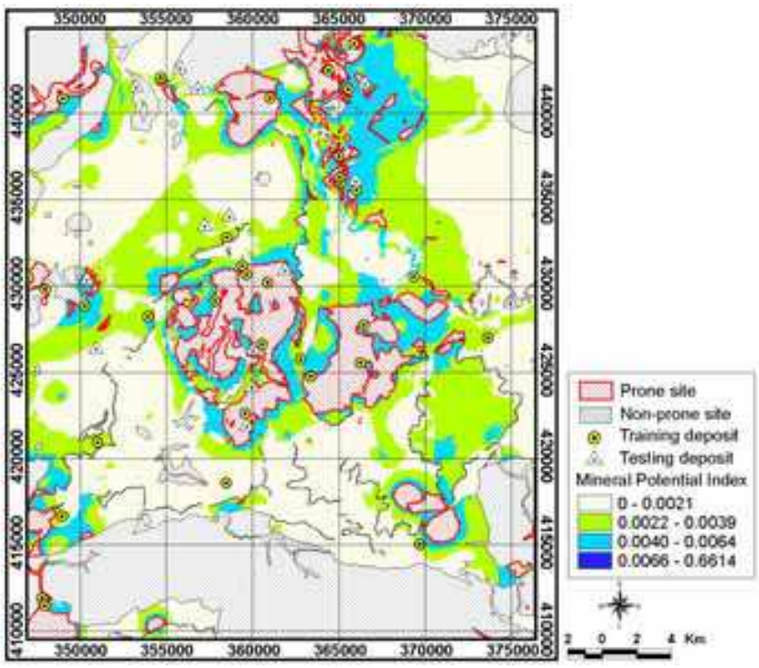

(c)

Fig. 5. Mineral potential maps based on likelihood ratio (a), weights of evidence (b) and logistic regression models (c): reclassification of low 60% (ivory colour), medium 20% (green colour), high 10% (sky blue colour), and very high 10% (blue colour) based on mineral potential index; training sites including "prone" (very high 10%) and "non-prone" (very low 10%) to deposit occurrence

5. Mineral deposit potential analysis using the Artificial Neural Network

The 26 factors were used as the input data. Nine cases of training sites of mineral deposit-prone locations and the locations that were not prone to mineral deposits were made (Table 2). It can be difficult to specifically estimate a criterion for selection of training sites using any predictor map because deposits are formed by various geological factors processes. Classification of location that is prone and non-prone to mineral deposits from expert's experience can also change and be subjective when more information is available. While cells including a known deposit are indubitably mineralized, cells that do not include a known deposit may or may not be mineralized. If small deposit and non-deposit training data are selected from the known deposit cell and the large corpus of non-deposit cell, respectively, the mineral potential map can be highly sensitive to particular choice of deposit and non-deposit training data (Skabar, 2005; Harris et al., 2003). Porwal et al., 2003 and Nykanen (2008) approached the problem of sensitivity of ANN to this non-deposit site training data by selecting training data in low mineral potential area modeled previously using a weights of evidence method. Skabar (2005) used for replicates of deposit locations. For each replicate set, they randomly selected and used 3/ 4 and 1/ 4 of the deposit locations for training and testing, respectively.

Models	Case	Prone area	Non-prone area
Likelihood ratio	Case 1	Deposit occurrence	10% areas with low mineral potential index (MPI_{LR})
	Case 2	5% areas with high mineral potential index (MPI_{LR})	10% areas with low mineral potential index (MPI_{LR})
	Case 3	10% areas with high mineral potential index (MPI_{LR})	10% areas with low mineral potential index (MPI_{LR})
Weights of evidence	Case 4	Deposit occurrence	10% areas with low mineral potential index (MPI_{WOE})
	Case 5	5% areas with high mineral potential index (MPI_{WOE})	10% areas with low mineral potential index (MPI_{WOE})
	Case 6	10% areas with high mineral potential index (MPI_{WOE})	10% areas with low mineral potential index (MPI_{LO})
Logistic regression	Case 7	Deposit occurrence	10% areas with low mineral potential index (MPI_{WOE})
	Case 8	5% areas with high mineral potential index (MPI_{LO})	10% areas with low mineral potential index (MPI_{LO})
	Case 9	10% areas with high mineral	10% areas with low mineral

Table 2. Nine different training cases determined from likelihood ratio, weights of evidence and logistic regression models

To select training sites based on scientific and objective criteria, we used values of MPI_{LR}, MPI_{WOE}, MPI_{LO} (Fig. 5) because they represent relationships of deposit- and non-deposit locations with various factors. Pixels from each of the two classes were randomly selected as training pixels, with 32 pixels denoting areas where training mineral deposits occurred.

	Case 1								Case 2									
Factors	Run1	Run2	Run3	Run4	Run5	Mean	S.D.	N.V.	Run1	Run2	Run3	Run4	Run5	Mean	S.D.	N.V.	Run1	Ru
Al	0.032	0.042	0.037	0.043	0.046	0.040	0.006	1.136	0.037	0.037	0.038	0.041	0.046	0.040	0.004	1.149	0.037	0.0
As	0.034	0.034	0.036	0.036	0.038	0.036	0.002	1.011	0.039	0.034	0.033	0.037	0.038	0.036	0.003	1.045	0.037	0.0
Ba	0.042	0.042	0.037	0.040	0.032	0.038	0.004	1.085	0.038	0.037	0.041	0.037	0.031	0.037	0.004	1.067	0.043	0.0
Ca	0.036	0.035	0.034	0.037	0.038	0.036	0.001	1.019	0.043	0.042	0.036	0.042	0.040	0.040	0.003	1.170	0.037	0.0
Cd	0.034	0.038	0.040	0.040	0.039	0.038	0.002	1.080	0.040	0.036	0.027	0.032	0.038	0.035	0.005	1.000	0.041	0.0
Cl^-	0.041	0.036	0.039	0.030	0.033	0.036	0.004	1.014	0.035	0.038	0.037	0.042	0.032	0.037	0.004	1.066	0.045	0.0
Co	0.041	0.034	0.038	0.038	0.039	0.038	0.003	1.068	0.039	0.037	0.035	0.037	0.040	0.038	0.002	1.084	0.040	0.0
Cr	0.040	0.038	0.035	0.035	0.033	0.036	0.003	1.027	0.042	0.044	0.047	0.038	0.035	0.041	0.005	1.190	0.032	0.0
Cu	0.037	0.039	0.041	0.035	0.047	0.040	0.004	1.130	0.038	0.045	0.038	0.035	0.048	0.041	0.005	1.173	0.045	0.0
F^-	0.039	0.044	0.044	0.040	0.036	0.041	0.004	1.148	0.031	0.042	0.045	0.041	0.035	0.039	0.006	1.120	0.043	0.0
Fe	0.029	0.038	0.035	0.040	0.037	0.036	0.004	1.010	0.039	0.039	0.034	0.035	0.037	0.037	0.002	1.061	0.037	0.0
K	0.037	0.036	0.036	0.033	0.044	0.037	0.004	1.047	0.035	0.037	0.041	0.036	0.043	0.039	0.003	1.115	0.033	0.0
Li	0.037	0.037	0.036	0.039	0.038	0.037	0.001	1.059	0.042	0.037	0.041	0.048	0.036	0.041	0.005	1.178	0.041	0.0
Mg	0.039	0.042	0.044	0.042	0.042	0.042	0.002	1.191	0.034	0.041	0.035	0.044	0.039	0.038	0.004	1.110	0.036	0.0
Mn	0.033	0.035	0.033	0.043	0.034	0.036	0.004	1.008	0.038	0.041	0.036	0.037	0.035	0.038	0.002	1.086	0.046	0.0
Na	0.041	0.031	0.043	0.033	0.035	0.036	0.005	1.026	0.041	0.038	0.045	0.044	0.036	0.041	0.004	1.176	0.031	0.0
Ni	0.053	0.047	0.039	0.046	0.045	0.046	0.005	1.294	0.050	0.048	0.036	0.040	0.046	0.044	0.006	1.270	0.036	0.0
Pb	0.040	0.035	0.043	0.036	0.040	0.039	0.003	1.101	0.043	0.045	0.036	0.042	0.042	0.042	0.003	1.204	0.037	0.0
Si	0.039	0.039	0.033	0.044	0.040	0.039	0.004	1.101	0.039	0.035	0.038	0.031	0.040	0.037	0.004	1.058	0.039	0.0
Sr	0.033	0.042	0.038	0.037	0.039	0.038	0.003	1.068	0.035	0.035	0.042	0.037	0.040	0.038	0.003	1.101	0.040	0.0
V	0.040	0.040	0.043	0.034	0.044	0.040	0.004	1.137	0.044	0.034	0.049	0.035	0.043	0.041	0.006	1.184	0.035	0.0
W	0.041	0.031	0.045	0.037	0.034	0.038	0.005	1.066	0.031	0.031	0.044	0.035	0.034	0.035	0.005	1.005	0.039	0.0
Zn	0.046	0.039	0.046	0.039	0.034	0.041	0.005	1.154	0.037	0.032	0.041	0.036	0.035	0.036	0.003	1.038	0.039	0.0
Mag.	0.039	0.046	0.037	0.040	0.035	0.039	0.004	1.111	0.034	0.038	0.036	0.043	0.035	0.037	0.004	1.076	0.039	0.0
Fault	0.040	0.045	0.036	0.049	0.043	0.043	0.005	1.205	0.040	0.039	0.034	0.032	0.043	0.037	0.004	1.083	0.036	0.0
Geology	0.038	0.036	0.035	0.035	0.034	0.035	0.002	1.000	0.038	0.039	0.038	0.043	0.034	0.038	0.003	1.109	0.038	0.0

	Case 4								Case 5									
Factors	Run1	Run2	Run3	Run4	Run5	Mean	S.D.	N.V.	Run1	Run2	Run3	Run4	Run5	Mean	S.D.	N.V.	Run1	Ru
Al	0.031	0.047	0.037	0.033	0.043	0.038	0.007	1.144	0.038	0.031	0.038	0.038	0.042	0.037	0.004	1.078	0.038	0.0
As	0.033	0.043	0.039	0.039	0.044	0.040	0.004	1.186	0.042	0.037	0.033	0.042	0.036	0.038	0.004	1.106	0.042	0.0
Ba	0.041	0.038	0.033	0.037	0.043	0.038	0.004	1.150	0.038	0.036	0.039	0.042	0.039	0.039	0.002	1.118	0.041	0.0
Ca	0.037	0.041	0.040	0.043	0.039	0.040	0.002	1.198	0.036	0.041	0.036	0.039	0.036	0.038	0.003	1.088	0.033	0.0
Cd	0.033	0.037	0.042	0.036	0.034	0.036	0.004	1.090	0.036	0.040	0.039	0.036	0.040	0.038	0.002	1.108	0.038	0.0
Cl^-	0.041	0.034	0.041	0.040	0.035	0.038	0.003	1.144	0.033	0.042	0.039	0.042	0.035	0.038	0.004	1.104	0.042	0.0

Co	0.039	0.036	0.039	0.040	0.037	0.038	0.002	1.144	0.037	0.040	0.037	0.033	0.044	0.038	0.004	1.110	0.030	0.0
Cr	0.039	0.039	0.040	0.035	0.042	0.039	0.003	1.168	0.037	0.033	0.034	0.043	0.036	0.036	0.004	1.054	0.038	0.0
Cu	0.036	0.045	0.033	0.039	0.049	0.040	0.007	1.210	0.041	0.034	0.042	0.037	0.034	0.037	0.004	1.085	0.038	0.0
F-	0.038	0.040	0.035	0.043	0.040	0.039	0.003	1.174	0.036	0.039	0.042	0.037	0.035	0.038	0.003	1.096	0.043	0.0
Fe	0.029	0.034	0.033	0.033	0.038	0.033	0.003	1.000	0.044	0.039	0.035	0.035	0.043	0.039	0.004	1.144	0.036	0.0
K	0.037	0.031	0.041	0.043	0.036	0.038	0.005	1.126	0.040	0.034	0.036	0.035	0.037	0.036	0.002	1.053	0.041	0.0
Li	0.038	0.041	0.039	0.034	0.037	0.038	0.003	1.132	0.045	0.038	0.040	0.044	0.037	0.041	0.003	1.182	0.036	0.0
Mg	0.037	0.036	0.043	0.039	0.032	0.037	0.004	1.120	0.041	0.038	0.042	0.037	0.041	0.040	0.002	1.148	0.033	0.0
Mn	0.033	0.044	0.039	0.039	0.041	0.039	0.004	1.174	0.046	0.047	0.033	0.036	0.043	0.041	0.006	1.182	0.043	0.0
Na	0.041	0.037	0.048	0.046	0.041	0.043	0.004	1.275	0.036	0.034	0.042	0.038	0.042	0.038	0.004	1.109	0.045	0.0
Ni	0.053	0.033	0.039	0.042	0.040	0.041	0.007	1.240	0.044	0.035	0.041	0.050	0.040	0.042	0.006	1.212	0.040	0.0
Pb	0.041	0.040	0.038	0.034	0.032	0.037	0.004	1.108	0.042	0.039	0.042	0.031	0.037	0.038	0.004	1.104	0.037	0.0
Si	0.038	0.037	0.031	0.030	0.031	0.033	0.004	1.000	0.028	0.037	0.033	0.036	0.044	0.036	0.006	1.035	0.042	0.0
Sr	0.033	0.037	0.041	0.036	0.035	0.036	0.003	1.090	0.046	0.039	0.037	0.035	0.037	0.039	0.004	1.123	0.036	0.0
V	0.039	0.034	0.036	0.033	0.038	0.036	0.003	1.078	0.037	0.045	0.041	0.043	0.030	0.039	0.006	1.133	0.041	0.0
W	0.045	0.046	0.047	0.047	0.038	0.045	0.004	1.335	0.036	0.039	0.045	0.038	0.037	0.039	0.004	1.129	0.045	0.0
Zn	0.046	0.037	0.031	0.036	0.037	0.037	0.005	1.120	0.034	0.041	0.047	0.039	0.039	0.040	0.005	1.158	0.033	0.0
Mag.	0.044	0.037	0.040	0.049	0.043	0.043	0.005	1.275	0.047	0.046	0.038	0.038	0.040	0.042	0.004	1.208	0.040	0.0
Fault	0.039	0.038	0.037	0.035	0.036	0.037	0.002	1.108	0.036	0.038	0.035	0.044	0.040	0.039	0.004	1.117	0.038	0.0
Geology	0.038	0.039	0.037	0.040	0.040	0.039	0.001	1.162	0.030	0.038	0.035	0.033	0.037	0.035	0.003	1.000	0.033	0.0
	Case 7								Case 8									
Factors	Run1	Run2	Run3	Run4	Run5	Mean	S.D.	N.V.	Run1	Run2	Run3	Run4	Run5	Mean	S.D.	N.V.	Run1	Ru
Al	0.038	0.034	0.040	0.038	0.037	0.037	0.002	1.081	0.034	0.036	0.038	0.041	0.039	0.038	0.002	1.180	0.038	0.0
As	0.035	0.048	0.042	0.042	0.040	0.041	0.005	1.192	0.042	0.042	0.047	0.051	0.042	0.045	0.004	1.413	0.040	0.0
Ba	0.040	0.032	0.033	0.034	0.035	0.035	0.003	1.000	0.038	0.034	0.046	0.037	0.040	0.039	0.004	1.227	0.040	0.0
Ca	0.044	0.039	0.038	0.036	0.041	0.040	0.003	1.144	0.032	0.038	0.034	0.035	0.036	0.035	0.002	1.095	0.033	0.0
Cd	0.036	0.039	0.036	0.039	0.038	0.037	0.002	1.084	0.034	0.034	0.034	0.038	0.039	0.036	0.002	1.133	0.042	0.0
Cl-	0.041	0.038	0.043	0.042	0.036	0.040	0.003	1.150	0.041	0.039	0.038	0.037	0.041	0.039	0.002	1.232	0.041	0.0
Co	0.041	0.042	0.040	0.038	0.037	0.040	0.002	1.150	0.042	0.042	0.044	0.038	0.041	0.041	0.002	1.296	0.037	0.0
Cr	0.040	0.038	0.041	0.042	0.043	0.041	0.002	1.178	0.037	0.036	0.036	0.041	0.036	0.037	0.002	1.168	0.036	0.0
Cu	0.041	0.035	0.037	0.046	0.038	0.039	0.004	1.136	0.035	0.036	0.040	0.039	0.038	0.037	0.002	1.173	0.036	0.0
F-	0.040	0.040	0.040	0.034	0.030	0.037	0.005	1.059	0.042	0.045	0.037	0.041	0.045	0.042	0.003	1.309	0.045	0.0
Fe	0.039	0.036	0.039	0.032	0.040	0.037	0.003	1.073	0.037	0.034	0.036	0.036	0.041	0.037	0.002	1.159	0.039	0.0
K	0.038	0.039	0.032	0.039	0.036	0.037	0.003	1.064	0.038	0.039	0.037	0.036	0.037	0.037	0.001	1.173	0.036	0.0
Li	0.043	0.040	0.040	0.036	0.041	0.040	0.003	1.160	0.041	0.041	0.041	0.031	0.033	0.037	0.005	1.172	0.030	0.0
Mg	0.041	0.037	0.037	0.040	0.034	0.038	0.003	1.093	0.037	0.039	0.041	0.040	0.034	0.038	0.003	1.196	0.037	0.0

Mn	0.037	0.039	0.040	0.039	0.041	0.039	0.001	1.134	0.035	0.036	0.038	0.039	0.040	0.037	0.002	1.176	0.040	0
Na	0.042	0.041	0.041	0.040	0.041	0.041	0.001	1.189	0.044	0.043	0.040	0.042	0.037	0.041	0.003	1.298	0.036	0
Ni	0.030	0.038	0.038	0.039	0.047	0.038	0.006	1.110	0.044	0.035	0.040	0.038	0.039	0.039	0.003	1.228	0.042	0
Pb	0.041	0.034	0.034	0.041	0.044	0.039	0.004	1.120	0.041	0.041	0.041	0.036	0.043	0.041	0.003	1.274	0.042	0
Si	0.038	0.041	0.033	0.030	0.038	0.036	0.004	1.039	0.033	0.040	0.037	0.038	0.040	0.038	0.003	1.178	0.038	0
Sr	0.040	0.045	0.042	0.039	0.035	0.040	0.004	1.164	0.040	0.047	0.036	0.044	0.049	0.043	0.005	1.354	0.043	0
V	0.034	0.034	0.040	0.041	0.044	0.038	0.004	1.112	0.044	0.043	0.039	0.036	0.030	0.038	0.006	1.200	0.042	0
W	0.030	0.044	0.033	0.038	0.029	0.035	0.006	1.010	0.043	0.038	0.033	0.033	0.035	0.036	0.004	1.142	0.048	0
Zn	0.039	0.040	0.043	0.040	0.039	0.040	0.002	1.161	0.037	0.037	0.027	0.027	0.031	0.032	0.005	1.000	0.037	0
Mag.	0.038	0.044	0.035	0.039	0.033	0.038	0.004	1.092	0.034	0.039	0.034	0.038	0.042	0.037	0.003	1.173	0.028	0
Fault	0.039	0.033	0.043	0.045	0.045	0.041	0.005	1.182	0.035	0.032	0.044	0.044	0.036	0.038	0.005	1.202	0.034	0
Geology	0.036	0.033	0.041	0.032	0.039	0.036	0.004	1.040	0.041	0.034	0.043	0.046	0.037	0.040	0.005	1.258	0.041	0

Mag.: Magnetic anomaly
S.D.: Standard deviation
N.V.: Normalized value divided by the minimum average weight

Table 3. Weight of artificial neural network in study area

The back-propagation algorithm was then applied to calculate the weights between the input layer and the hidden layer, and between the hidden layer and the output layer, by modifying the number of hidden node and the learning rate. A three-layered feed-forward network was implemented using the MATLAB software package based on the framework provided by Hines (1997). Here, "feed-forward" denotes that the interconnections between the layers propagate forward to the next layer. The number of hidden layers and the number of nodes in a hidden layer required for a particular classification problem are not easy to deduce. In this study, a 26 x 52 x 2 structure was selected for the network, with input data normalized in the range 0.0-1.0. The nominal and interval class group data were converted to continuous values ranging between 0.0 and 1.0. Therefore, the continuous values were not ordinal data, but nominal data, and the numbers denote the classification of the input data. The learning rate was set to 0.01, and the initial weights were randomly selected to values between 0.1 and 0.3. The weights calculated from 5 test cases were compared to determine whether the variation in the final weights was dependent on the selection of the initial weights (Table 3).

The results show that the initial weights did not have an influence on the final weight under the conditions used. The back-propagation algorithm was used to minimize the error between the predicted output values and the calculated output values. The algorithm propagated the error backwards, and iteratively adjusted the weights. The number of epochs was set to 5,000, and the root mean square error (RMSE) value used for the stopping criterion was set to 0.01. Most of the training data sets met the 0.01 RMSE goal. However, if the RMSE value was not achieved, then the maximum number of iterations was terminated at 5,000 epochs. When the latter case occurred, then the maximum RMSE value was <0.2.

The final weights between layers acquired during training of the neural network and the contribution or importance of each of the 26 factors used to predict mineral deposit potential are shown in Table 3. The results were not the same, as the initial weights were assigned random values. Therefore, in this study, the calculations were repeated 5 times, to allow the results to achieve similar values. For easy interpretation, the average values were calculated, and these values were divided by the average of the weights of the some factor that had a minimum value. For Case 1, the geology value was the minimum value, 1.00, and the Ni was the maximum value, 1.294. For Case 2, the Cd value was the minimum value, 1.00, and the Ni was the maximum value, 1.270. For Case 3, the K value was the minimum value, 1.00, and the Cl- was the maximum value, 1.254. For Case 4, the Fe value was the minimum value, 1.00, and the W was the maximum value, 1.335. For Case 5, the geology value was the minimum value, 1.00, and the Ni was the maximum value, 1.212. For Case 6, the Pb value was the minimum value, 1.00, and the F- was the maximum value, 1.197. For Case 7, the Ba value was the minimum value, 1.00, and the As was the maximum value, 1.192. For Case 8, the Zn value was the minimum value, 1.00, and the As was the maximum value, 1.413. For Case 9, the magnetic value was the minimum value, 1.00, and the Pb was the maximum value, 1.317. The standard deviations of the results for all cases were in the range 0.001–0.008, and therefore, the random sampling did not have a large effect on the results. As the result, the As value was the minimum value, 1.00, and the Si was the maximum value, 1.1829. Finally, the weights were applied to the entire study area, and the mineral deposit potential maps were created for each training cases (Fig. 6).

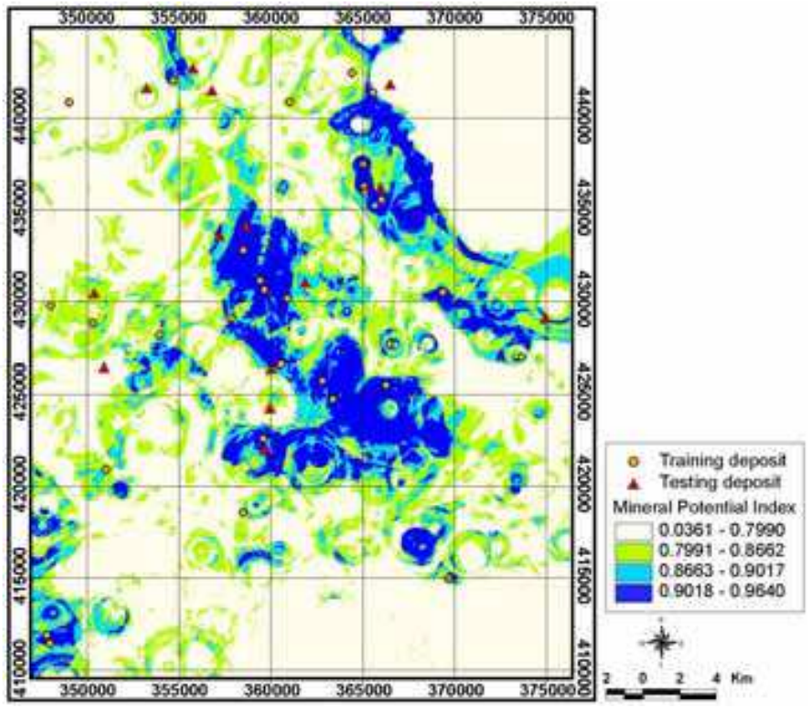

(a) Case 1

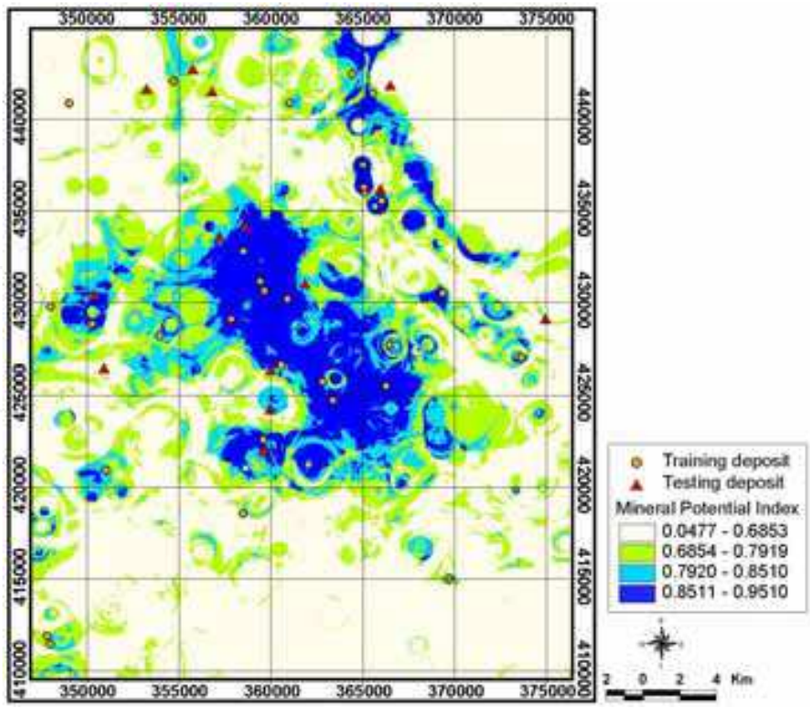

(b) Case 2

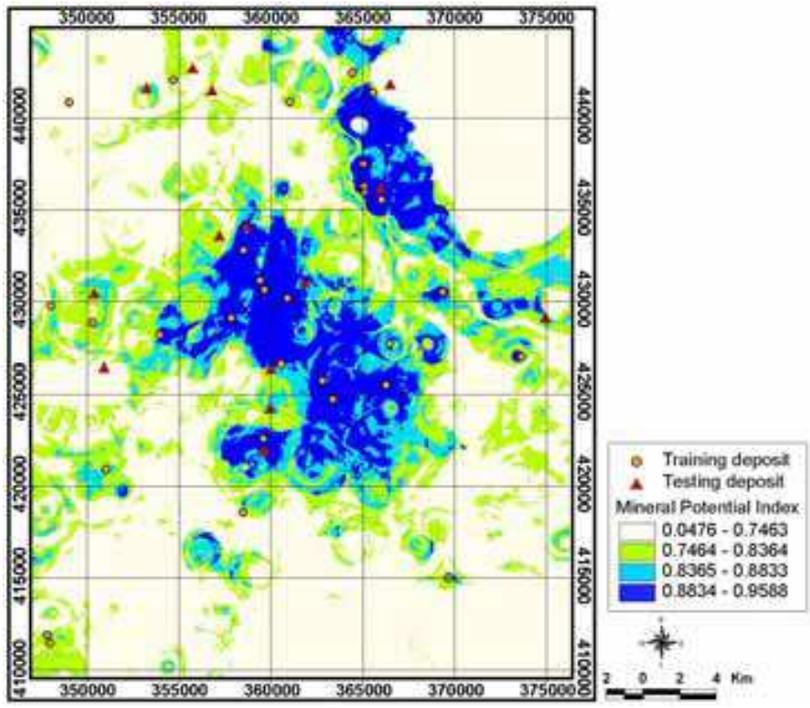

(c) Case 3

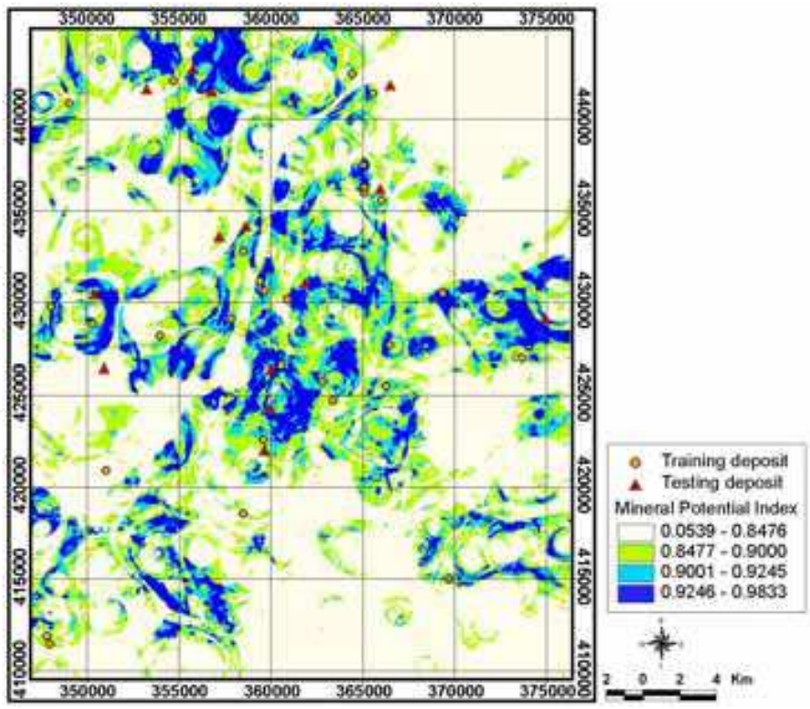

(d) Case 4

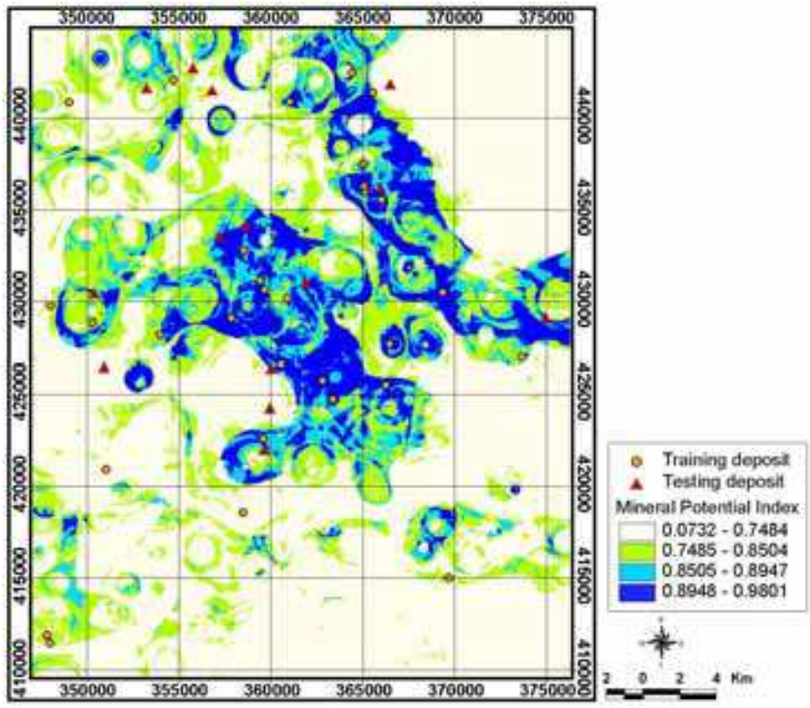

(e) Case 5

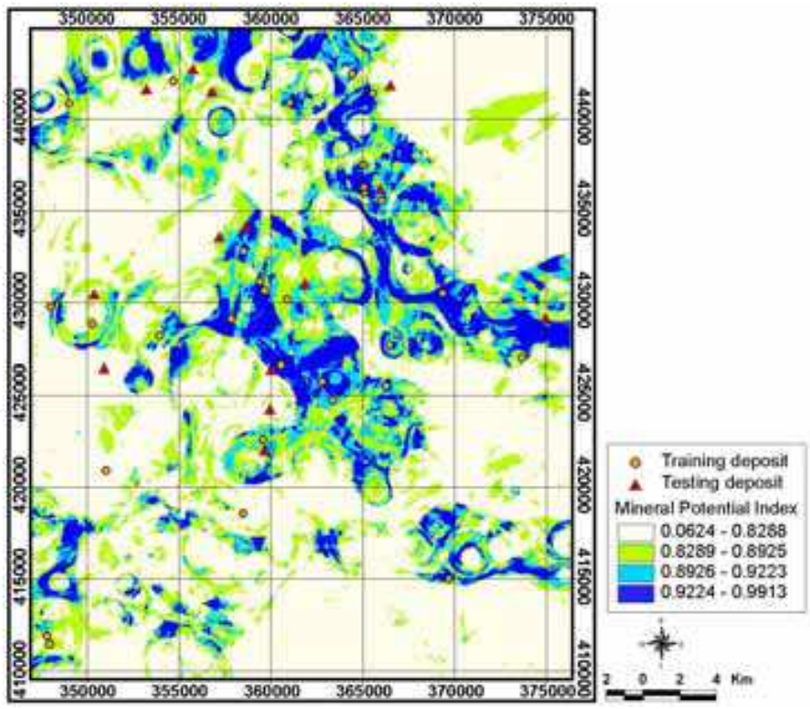

(f) Case 6

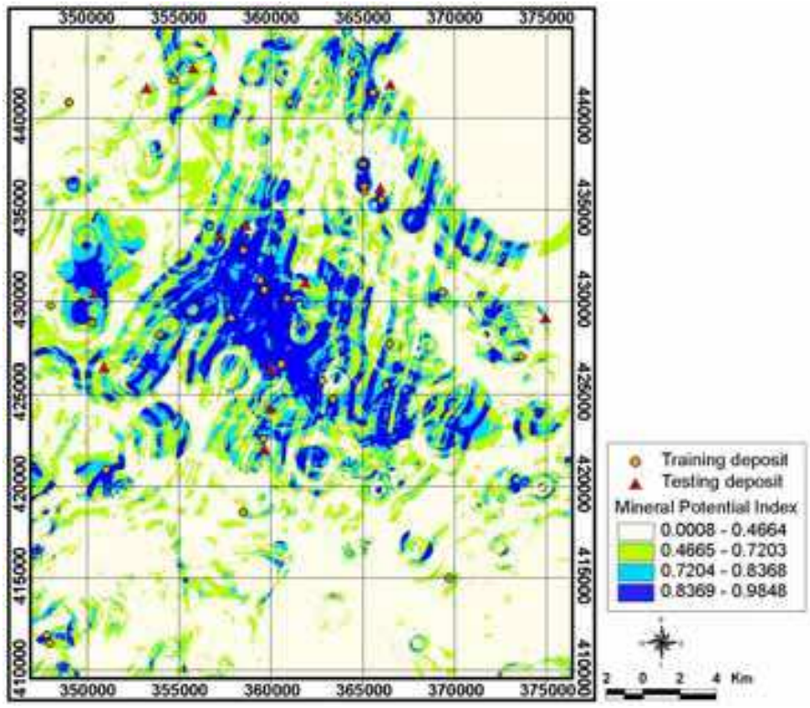

(g) Case 7

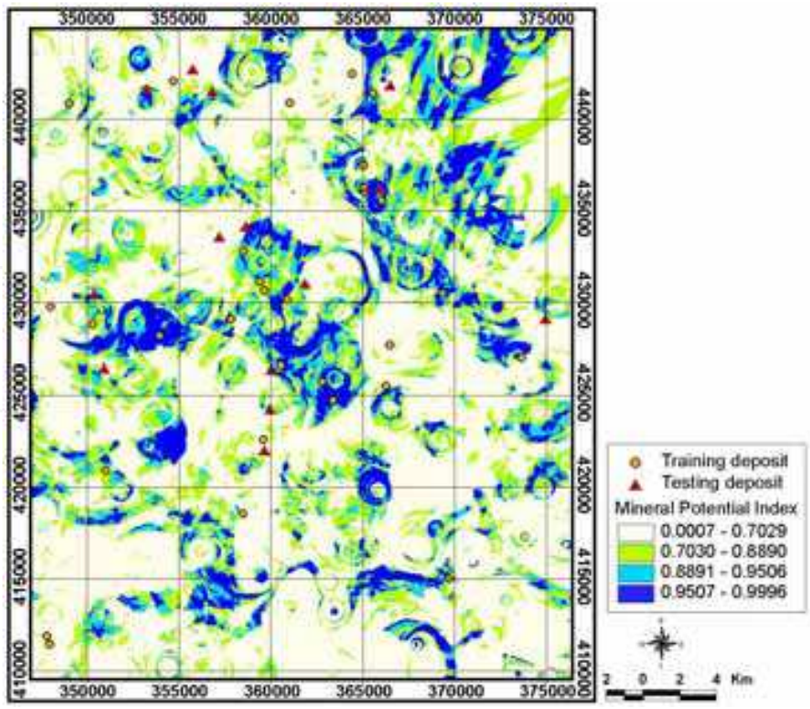

(h) Case 8

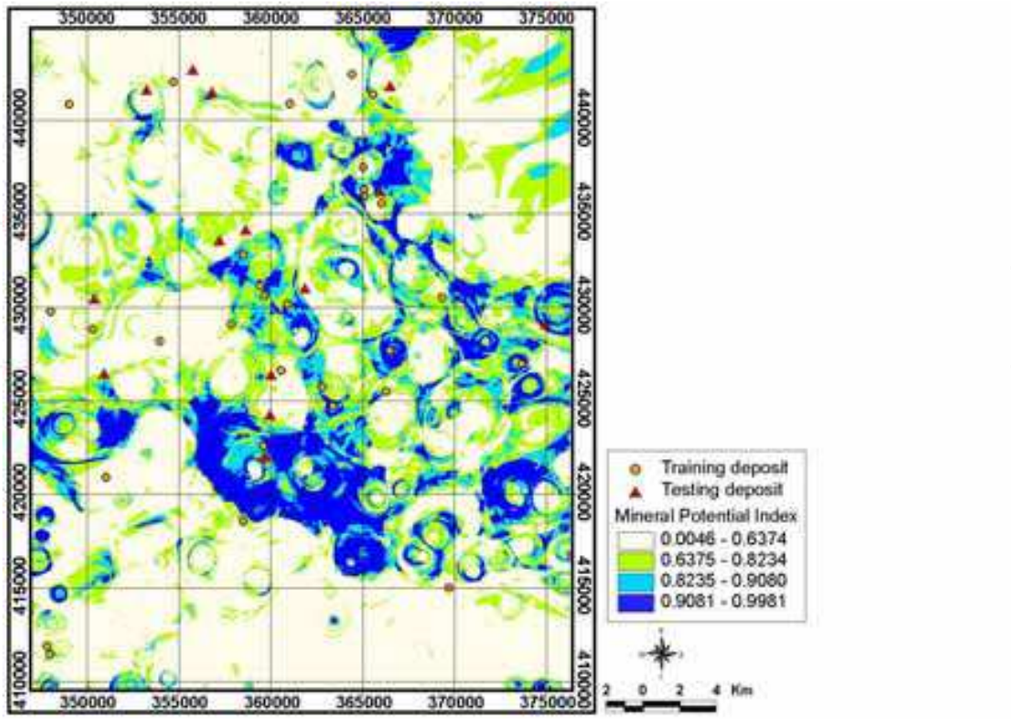

(i) Case 9

Fig. 6. Predictive gold-silver mineral potential map generated by reclassification of low 60% (ivory colour), medium 20% (green colour), high 10% (sky blue colour), and very high 10% (blue colour) based on mineral potential index; Case 1 (a), Case 2 (b), Case 3 (c), Case 4 (d) Case 5 (e), Case 6 (f), Case 7 (g), Case 8 (h) and Case 9 (i)

6. Validation

The mineral potential maps were validated by comparison with known mineral deposit locations (test set: 30% of total deposit) which were not used during the training of the artificial neural network model. For this, the success rate curves were calculated for quantitative prediction and area of under the curves was calculated. The rate shows how well the model and factors predict the mineral deposit occurrence. Thus, the area beneath the curve qualitatively assesses the prediction accuracy. To obtain the relative ranking for each prediction pattern, the calculated index values of all the pixels in the study area were sorted in descending order. The ordered pixel values were then divided into 100 classes with accumulated 1% intervals. The validation rate appears as a graph (Fig. 7).

For Case 1, Case 2, Case 3, Case 4, Case 5, Case 6, Case 7, Case 8 and Case 9, the 80–100% class (20%) in which the mineral potential index had a high rank could explain 56%, 50%, 56%, 56%, 56%, 50%, 44%, 25% and 44% of all the mineral deposit occurrences, respectively. The graphs shown are the best prediction accuracy among the five running.

To compare the result quantitatively, the areas under the curve were re-calculated as if the total area were one, which indicates perfect prediction accuracy. The area beneath a curve can therefore be used to assess the prediction accuracy qualitatively. For Case 1, Case 2, Case 3, Case 4, Case 5, Case 6, Case 7, Case 8 and Case 9, the area ratio was 0.7406, 0.7459,

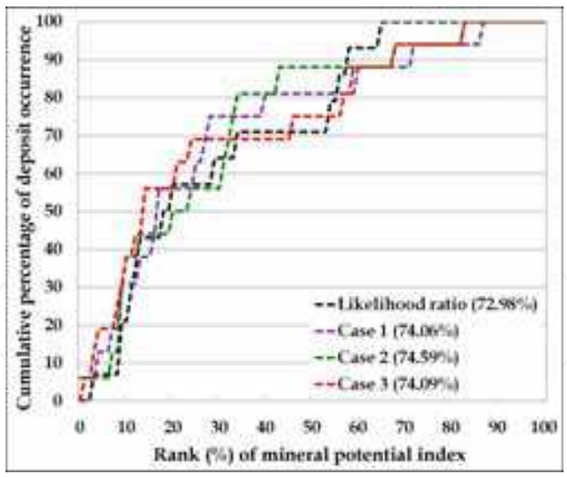

(a)

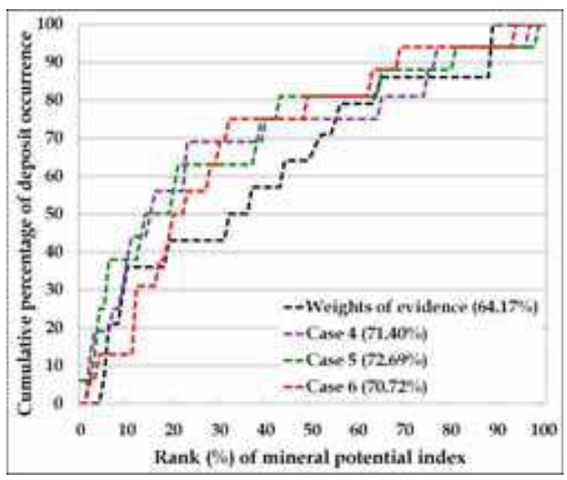

(b)

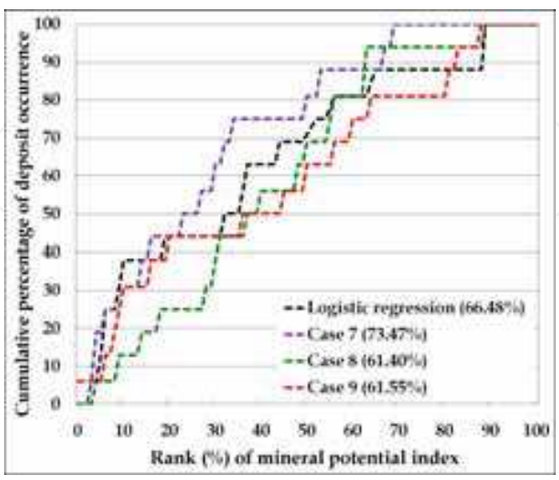

(c)

Fig. 7. Illustration of cumulative frequency diagram showing rank (%) of mineral potential index (x-axis) occurring in cumulative percent of mineral deposit occurrence (y-axis)

0.7409, 0.7140, 0.7269, 0.7072, 0.7347, 0.6140 and 0.6155 meaning a prediction accuracy of 74.06%, 74.59%, 74.09%, 71.40%, 72.69%, 70.72%, 73.47%, 61.40% and 61.55%.

7. Conclusion

Training sites were extracted from mineral potential maps based on likelihood ratio, weights of evidence and logistic regression methods, which showed 72.98%, 64.71% and 66.48% prediction accuracy validated by the test set. In the study, the mineral potential map of gold-silver were made using the artificial neural network and nine cases of training sites, each of which consist of 32 locations randomly selected among known mineral occurrences in 5% and 10% of areas with the high mineral potential index values and 32 non-deposit locations randomly selected in 10% of areas with low mineral potential index. The validation result of Case 1, Case 2, Case 3, Case 4, Case 5, Case 6, Case 7, Case 8 and Case 9 showed, respectively, the 74.06%, 74.59%, 74.09%, 71.40%, 72.69%, 70.72%, 73.47%, 61.40% and 61.55% prediction accuracy using 14 test mineral deposits not used directly for the analysis. All training cases exhibited accuracies of over 70% but Cases 8 and 9, slightly higher or lower than likelihood ratio and very higher than weights of evidence and logistic regression models. Overall, training cases based on likelihood ratio model, gave higher accuracies than training cases based on weights of evidence and logistic regression models. This result shows that some of the testing deposits plotted in non-prone area to deposit occurrence (Figs. 5b and 5c), and the weights of evidence and logistic regression represented the low accuracy among the methods. However, the analysis result of some training sets shows more sensitive to training data by logistic regression than weighs of evidence.

Some researches approached a degree of sensitivity by selecting non-deposit site training data in low-probability area of previously generated potential maps made using weights of evidence or/ and logistic regression (Porwal et al., 2003; Behnia, 2007; Nykanen & Salmirinne, 2007; Nykanen, 2008). Using larger training data reduces the variance of initial weight in the ANN and improves accuracy of the resulting potential map (Skabar, 2005; Nykanen, 2008). In the study, 32 deposit and non-deposit cells were represented equally in the training set, although, the network to training data was repeated five times to reduce sensitive to initial weights of factors related to gold-silver mineral.

The resulting map by ANN can be possible to show better prediction accuracy if training dataset are selected from MPM with more high accuracy than MPM by likelihood ratio in the study. A Geographic Information System (GIS), in concert with artificial neural network software was used to compile, manipulate, analyze and visualize a large geological, geochemical and geophysical dataset collected from the Taebaeksan mineralized district of Eastern Korea. The GIS is not only capable of routine display, but also offer great potential by providing a range of tools to query, manipulate, visualize and analyze geological, geochemical and geophysical data in mineral exploration applications. The artificial neural network that was applied to the logistic sigmoid transfer function proved useful for predicting and evaluating the mineral potential map produced in this study. The models are useful for providing a quantitative measure of the weights among the factors for gold-silver prospects. Furthermore, the maps generated by the models, not only predict known areas of gold-silver occurrence, but also identify areas of potential mineralization where no known deposit occurs. Several areas within the study area are identified as having high gold-silver potential. Many of these areas coincide with areas of known deposits.

8. Appendixes

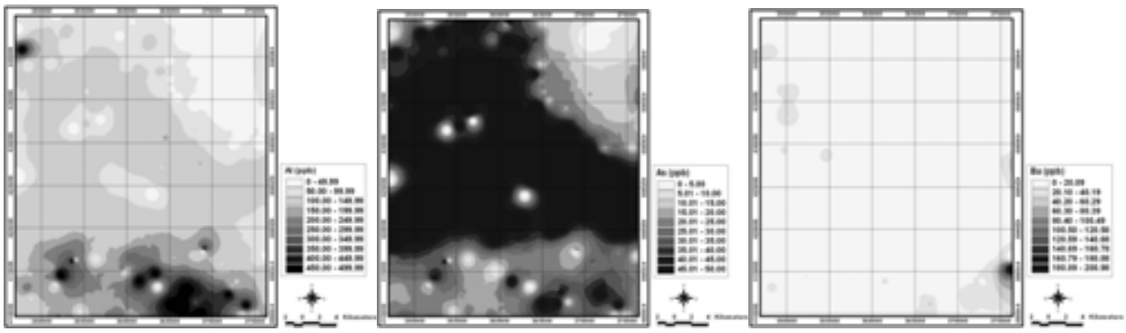

(a) Al (b) As (c) Ba

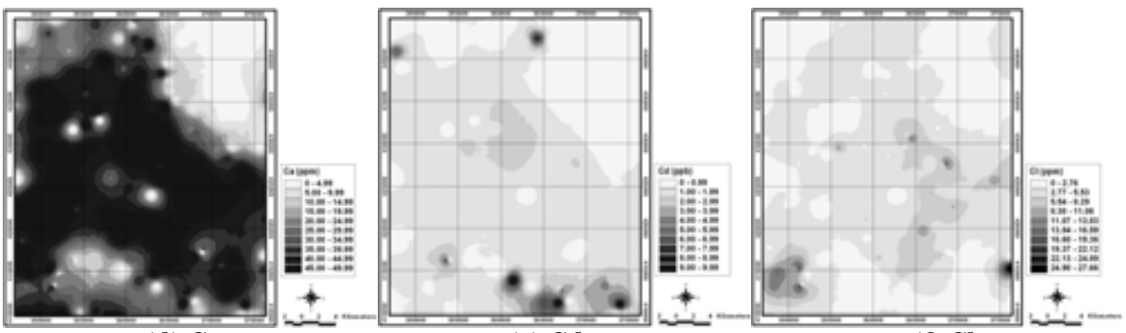

(d) Ca (e) Cd (f) Cl^-

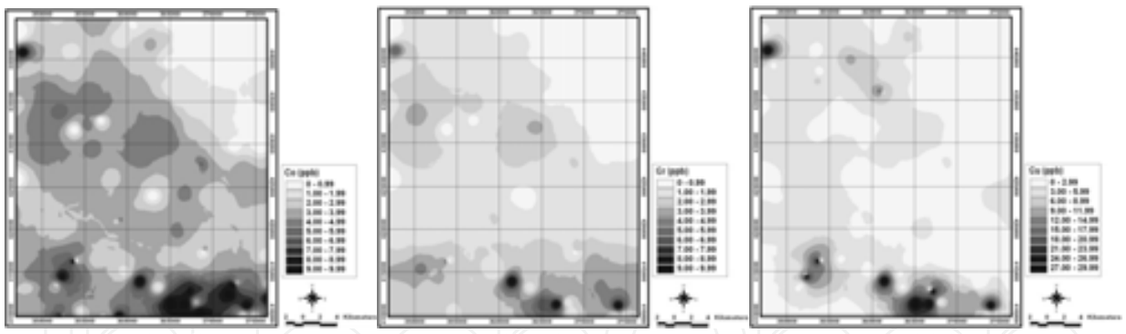

(g) Co (h) Cr (i) Cu

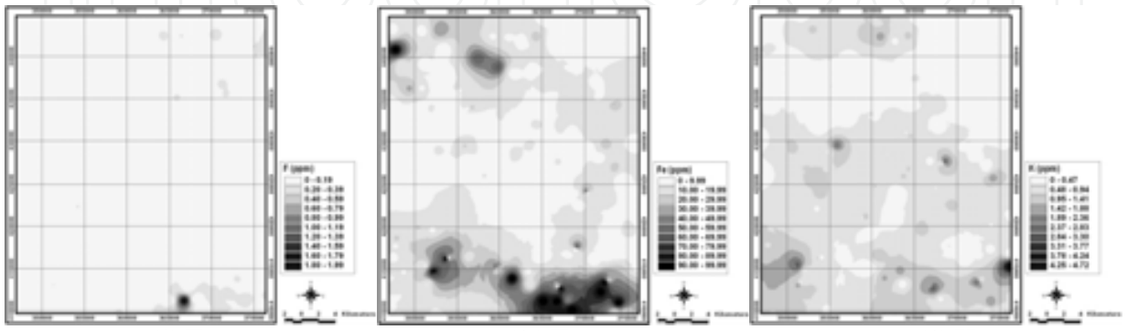

(j) F^- (k) Fe (l) K

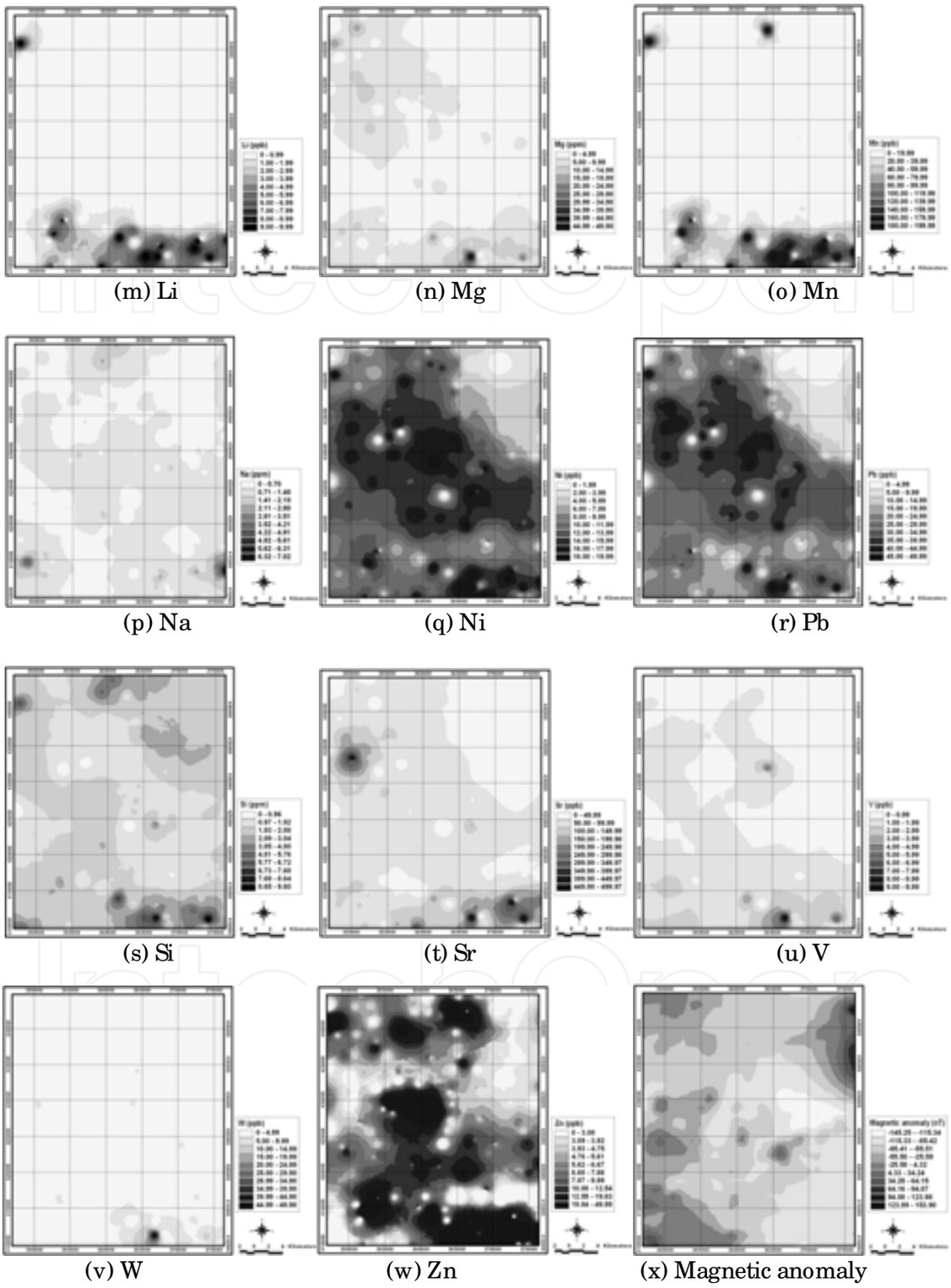

Fig. A1. Geochemical (Lee et al., 1998) and magnetic anomaly (Koo et al., 2001) maps

Factor	Likelihood ratio						Weights of evidence				Logistic regression
	Class [a]	No. of pixels	%Area	Mineral occ.	%occ.	LS [b]	W+	W-	C	C/ S(c)	Coefficient [c]
Al (ppb)	26.00-44.15	116666	10.00	3	9.38	0.94	-0.06	0.01	-0.07	-0.12	0.00806
	44.16-84.54	116651	10.00	3	9.38	0.94	-0.06	0.01	-0.07	-0.12	
	84.55-103.39	116737	10.01	4	12.50	1.25	0.22	-0.03	0.25	0.47	
	103.40-112.87	116716	10.01	2	6.25	0.62	-0.47	0.04	-0.51	-0.70	
	112.88-119.29	116695	10.00	7	21.88	2.19	0.78	-0.14	0.92	2.16	
	119.30-124.97	116601	10.00	7	21.88	2.19	0.78	-0.14	0.92	2.16	
	124.98-133.04	116613	10.00	1	3.13	0.31	-1.16	0.07	-1.24	-1.22	
	133.05-164.69	116594	10.00	3	9.38	0.94	-0.06	0.01	-0.07	-0.12	
	164.70-231.11	116586	10.00	2	6.25	0.63	-0.47	0.04	-0.51	-0.70	
	231.12-499.99	116579	9.99	0	0.00	0.00	NaN	0.11	NaN	NaN	
As (ppm)	1.01-14.58	116689	10.00	0	0.00	0.00	NaN	0.11	NaN	NaN	0.03186
	14.59-21.78	116779	10.01	8	25.00	2.50	0.92	-0.18	1.10	2.69	
	21.79-27.56	116734	10.01	0	0.00	0.00	NaN	0.11	NaN	NaN	
	27.57-35.09	116702	10.00	3	9.38	0.94	-0.07	0.01	-0.07	-0.12	
	35.10-43.43	116782	10.01	1	3.13	0.31	-1.16	0.07	-1.24	-1.22	
	43.44-47.59	116901	10.02	4	12.50	1.25	0.22	-0.03	0.25	0.47	
	47.60-49.47	116516	9.99	0	0.00	0.00	NaN	0.11	NaN	NaN	
	49.48-49.99	65606	5.62	3	9.38	1.67	0.51	-0.04	0.55	0.91	
	50.00	283729	24.32	13	40.63	1.67	0.51	-0.24	0.76	2.10	
Ba (ppb)	2.00-3.99	117477	10.07	0	0.00	0.00	NaN	0.11	NaN	NaN	0.04983
	4.00-5.96	116734	10.01	8	25.00	2.50	0.92	-0.18	1.10	0.41	
	5.97-7.04	117258	10.05	2	6.25	0.62	-0.48	0.04	-0.52	0.73	
	7.05-7.86	116532	9.99	3	9.38	0.94	-0.06	0.01	-0.07	0.61	
	7.87-8.55	116787	10.01	5	15.63	1.56	0.45	-0.06	0.51	0.49	
	8.56-9.61	116822	10.02	4	12.50	1.25	0.22	-0.03	0.25	0.53	
	9.62 -10.87	116583	9.99	3	9.38	0.94	-0.06	0.01	-0.07	0.61	
	10.88-13.28	116120	9.96	1	3.13	0.31	-1.16	0.07	-1.23	1.02	
	13.29-17.38	116242	9.97	3	9.38	0.94	-0.06	0.01	-0.07	0.61	
	17.39-200.97	115883	9.93	3	9.38	0.94	-0.06	0.01	-0.06	0.61	
Ca (ppm)	1.53-6.24	116712	10.01	2	6.25	0.62	-0.47	0.04	-0.51	0.73	-0.00001
	6.25-18.99	116637	10.00	5	15.63	1.56	0.45	-0.06	0.51	0.49	
	19.00-28.24	116714	10.01	1	3.13	0.31	-1.16	0.07	-1.24	1.02	
	28.25-35.41	116742	10.01	3	9.38	0.94	-0.07	0.01	-0.07	0.61	
	35.42-40.44	116662	10.00	2	6.25	0.62	-0.47	0.04	-0.51	0.73	
	40.45-43.42	116679	10.00	2	6.25	0.62	-0.47	0.04	-0.51	0.73	
	43.43-46.01	116621	10.00	3	9.38	0.94	-0.06	0.01	-0.07	0.61	
	46.02-48.04	117223	10.05	4	12.50	1.24	0.22	-0.03	0.25	0.53	
	48.05-49.16	116647	10.00	5	15.63	1.56	0.45	-0.06	0.51	0.49	
	49.17-50.00	115801	9.93	5	15.63	1.57	0.45	-0.07	0.52	0.49	
Cd (ppm)	1.0000-1.1008	116740	10.01	3	9.38	0.94	-0.07	0.01	-0.07	0.61	-0.12562
	1.1009-1.2239	116647	10.00	3	9.38	0.94	-0.06	0.01	-0.07	0.61	
	1.2240-1.3473	116690	10.00	2	6.25	0.62	-0.47	0.04	-0.51	0.73	

	1.3474-1.4928	116699	10.00	3	9.38	0.94	-0.07	0.01	-0.07	0.61	
	1.4929-1.6538	116626	10.00	5	15.63	1.56	0.45	-0.06	0.51	0.49	
	1.6539-1.8480	116640	10.00	4	12.50	1.25	0.22	-0.03	0.25	0.53	
	1.8481-1.9829	116621	10.00	2	6.25	0.63	-0.47	0.04	-0.51	0.73	
	1.9830-2.2506	116610	10.00	5	15.63	1.56	0.45	-0.06	0.51	0.49	
	2.2507-3.2164	116585	9.99	1	3.13	0.31	-1.16	0.07	-1.24	1.02	
	3.2165-9.9992	116580	9.99	4	12.50	1.25	0.22	-0.03	0.25	0.53	
Cl- (ppm)	1.0106-2.2074	116644	10.00	1	3.13	0.31	-1.16	0.07	-1.24	1.02	0.00005
	2.2075-2.4546	116681	10.00	0	0.00	0.00	NaN	0.11	NaN	NaN	
	2.4547-2.7386	116654	10.00	3	9.38	0.94	-0.06	0.01	-0.07	0.61	
	2.7387-2.9874	116642	10.00	4	12.50	1.25	0.22	-0.03	0.25	0.53	
	2.9875-3.2353	116647	10.00	1	3.13	0.31	-1.16	0.07	-1.24	1.02	
	3.2354-3.4804	116642	10.00	7	21.88	2.19	0.78	-0.14	0.92	0.43	
	3.4805-3.8803	116637	10.00	5	15.63	1.56	0.45	-0.06	0.51	0.49	
	3.8804-4.7479	116635	10.00	5	15.63	1.56	0.45	-0.06	0.51	0.49	
	4.7480-5.9843	116628	10.00	2	6.25	0.63	-0.47	0.04	-0.51	0.73	
	5.9844-27.6669	116628	10.00	4	12.50	1.25	0.22	-0.03	0.25	0.53	
Co (ppb)	1.0000-1.5665	116648	10.00	4	12.50	1.25	0.22	-0.03	0.25	0.53	-0.51670
	1.5666-2.5807	116657	10.00	1	3.13	0.31	-1.16	0.07	-1.24	1.02	
	2.5808-1.9789	116722	10.01	6	18.75	1.87	0.63	-0.10	0.73	0.45	
	1.9790-3.1012	116636	10.00	1	3.13	0.31	-1.16	0.07	-1.24	1.02	
	3.1013-3.3506	116651	10.00	3	9.38	0.94	-0.06	0.01	-0.07	0.61	
	3.3507-3.6660	116656	10.00	2	6.25	0.62	-0.47	0.04	-0.51	0.73	
	3.6661-3.9952	116621	10.00	5	15.63	1.56	0.45	-0.06	0.51	0.49	
	3.9953-4.4250	116620	10.00	7	21.88	2.19	0.78	-0.14	0.92	0.43	
	4.4251-5.0758	116620	10.00	2	6.25	0.63	-0.47	0.04	-0.51	0.73	
	5.0759-9.9999	116607	10.00	1	3.13	0.31	-1.16	0.07	-1.24	1.02	
Cr (ppb)	1.0000-1.1958	116649	10.00	6	18.75	1.87	0.63	-0.10	0.73	0.45	-0.01601
	1.1959-1.3244	116645	10.00	0	0.00	0.00	NaN	0.11	NaN	NaN	
	1.3245-1.4319	116772	10.01	2	6.25	0.62	-0.47	0.04	-0.51	0.73	
	1.4320-1.5656	116663	10.00	6	18.75	1.87	0.63	-0.10	0.73	0.45	
	1.5657-1.8305	116650	10.00	4	12.50	1.25	0.22	-0.03	0.25	0.53	
	1.8306-2.0343	116653	10.00	3	9.38	0.94	-0.06	0.01	-0.07	0.61	
	2.0344-2.3185	116625	10.00	4	12.50	1.25	0.22	-0.03	0.25	0.53	
	2.3186-2.7629	116602	10.00	1	3.13	0.31	-1.16	0.07	-1.24	1.02	
	2.7630-3.2865	116601	10.00	6	18.75	1.88	0.63	-0.10	0.73	0.45	
	3.2866-9.9987	116578	9.99	0	0.00	0.00	NaN	0.11	NaN	NaN	
Cu (ppb)	1.000-2.034	116889	10.02	1	3.13	0.31	-1.17	0.07	-1.24	1.02	-0.50809
	2.035-2.450	116787	10.01	4	12.50	1.25	0.22	-0.03	0.25	0.53	
	2.451-2.744	116603	10.00	5	15.63	1.56	0.45	-0.06	0.51	0.49	
	2.745-2.994	117174	10.05	6	18.75	1.87	0.62	-0.10	0.73	0.45	
	2.995-3.262	116784	10.01	6	18.75	1.87	0.63	-0.10	0.73	0.45	
	3.263-3.669	116566	9.99	2	6.25	0.63	-0.47	0.04	-0.51	0.73	
	3.670-3.977	116422	9.98	4	12.50	1.25	0.23	-0.03	0.25	0.53	
	3.978-4.710	116412	9.98	2	6.25	0.63	-0.47	0.04	-0.51	0.73	
	4.711-7.695	116407	9.98	1	3.13	0.31	-1.16	0.07	-1.23	1.02	
	7.696-2.9999	116394	9.98	1	3.13	0.31	-1.16	0.07	-1.23	1.02	

F- (ppm)	0.03-0.14	117101	10.04	6	18.75	1.87	0.62	-0.10	0.73	0.45	-0.01003
	0.15-0.15	116775	10.01	2	6.25	0.62	-0.47	0.04	-0.51	0.73	
	0.16-0.16	117073	10.04	3	9.38	0.93	-0.07	0.01	-0.08	0.61	
	0.17-0.17	117348	10.06	3	9.38	0.93	-0.07	0.01	-0.08	0.61	
	0.18-0.18	117148	10.04	2	6.25	0.62	-0.47	0.04	-0.52	0.73	
	0.19-0.20	116558	9.99	5	15.63	1.56	0.45	-0.06	0.51	0.49	
	0.21-0.22	116117	9.95	4	12.50	1.26	0.23	-0.03	0.26	0.53	
	0.23-0.24	116151	9.96	3	9.38	0.94	-0.06	0.01	-0.07	0.61	
	0.25-0.28	116321	9.97	3	9.38	0.94	-0.06	0.01	-0.07	0.61	
	0.29-1.99	115846	9.93	1	3.13	0.31	-1.16	0.07	-1.23	1.02	
Fe (ppm)	2.00-6.77	117031	10.03	2	6.25	0.62	-0.47	0.04	-0.51	0.73	0.00002
	6.78-7.86	116771	10.01	5	15.63	1.56	0.45	-0.06	0.51	0.49	
	7.87-8.88	116611	10.00	5	15.63	1.56	0.45	-0.06	0.51	0.49	
	8.89-9.91	117384	10.06	4	12.50	1.24	0.22	-0.03	0.24	0.53	
	9.92-11.12	116592	10.00	6	18.75	1.88	0.63	-0.10	0.73	0.45	
	11.13-12.99	116876	10.02	1	3.13	0.31	-1.17	0.07	-1.24	1.02	
	13.00-15.76	116535	9.99	2	6.25	0.63	-0.47	0.04	-0.51	0.73	
	15.77-21.24	116233	9.96	3	9.38	0.94	-0.06	0.01	-0.07	0.61	
	21.25-35.77	116234	9.96	3	9.38	0.94	-0.06	0.01	-0.07	0.61	
	35.78-99.99	116171	9.96	1	3.13	0.31	-1.16	0.07	-1.23	1.02	
K (ppm)	0.1201-0.3403	116712	10.01	2	6.25	0.62	-0.47	0.04	-0.51	0.73	-0.00053
	0.3404-0.4005	116798	10.01	1	3.13	0.31	-1.16	0.07	-1.24	1.02	
	0.4006-0.4634	116644	10.00	5	15.63	1.56	0.45	-0.06	0.51	0.49	
	0.4635-0.5461	116707	10.01	2	6.25	0.62	-0.47	0.04	-0.51	0.73	
	0.5462-0.6365	116600	10.00	5	15.63	1.56	0.45	-0.06	0.51	0.49	
	0.6366-0.7389	116663	10.00	4	12.50	1.25	0.22	-0.03	0.25	0.53	
	0.7390-0.8133	116604	10.00	5	15.63	1.56	0.45	-0.06	0.51	0.49	
	0.8134-0.9078	116604	10.00	3	9.38	0.94	-0.06	0.01	-0.07	0.61	
	0.9079-1.0807	116575	9.99	2	6.25	0.63	-0.47	0.04	-0.51	0.73	
	10.808-4.7295	116531	9.99	3	9.38	0.94	-0.06	0.01	-0.07	0.61	
Li (ppb)	1.0000-1.0041	116661	10.00	6	18.75	1.87	0.63	-0.10	0.73	0.45	-0.22232
	1.0042-1.1144	116662	10.00	10	31.25	3.12	1.14	-0.27	1.41	0.38	
	1.1145-1.2670	116704	10.01	4	12.50	1.25	0.22	-0.03	0.25	0.53	
	1.2671-1.4984	116661	10.00	0	0.00	0.00	NaN	0.11	NaN	NaN	
	1.4985-1.9352	116631	10.00	2	6.25	0.63	-0.47	0.04	-0.51	0.73	
	1.9353-2.6544	116633	10.00	3	9.38	0.94	-0.06	0.01	-0.07	0.61	
	2.6545-3.5996	116624	10.00	3	9.38	0.94	-0.06	0.01	-0.07	0.61	
	3.5997-4.7935	116622	10.00	2	6.25	0.63	-0.47	0.04	-0.51	0.73	
	4.7936-6.6524	116623	10.00	1	3.13	0.31	-1.16	0.07	-1.24	1.02	
	6.6525-9.9999	116617	10.00	1	3.13	0.31	-1.16	0.07	-1.24	1.02	
Mg (ppm)	0.36-1.12	116873	10.02	0	0.00	0.00	NaN	0.11	NaN	NaN	-0.00001
	1.13-2.50	117756	10.10	8	25.00	2.48	0.91	-0.18	1.09	0.41	
	2.51-3.04	118493	10.16	4	12.50	1.23	0.21	-0.03	0.23	0.53	
	3.05-3.64	117481	10.07	3	9.38	0.93	-0.07	0.01	-0.08	0.61	
	3.65-4.41	116189	9.96	1	3.13	0.31	-1.16	0.07	-1.23	1.02	
	4.42-5.26	116652	10.00	5	15.63	1.56	0.45	-0.06	0.51	0.49	
	5.27-6.18	116279	9.97	4	12.50	1.25	0.23	-0.03	0.25	0.53	

	6.19-7.30	115792	9.93	5	15.63	1.57	0.45	-0.07	0.52	0.49	
	7.31-9.32	115912	9.94	1	3.13	0.31	-1.16	0.07	-1.23	1.02	
	9.33-49.99	115011	9.86	1	3.13	0.32	-1.15	0.07	-1.22	1.02	
Mn (ppb)	1.00-1.26	118658	10.17	4	12.50	1.23	0.21	-0.03	0.23	0.53	0.02688
	1.27-1.60	117500	10.07	2	6.25	0.62	-0.48	0.04	-0.52	0.73	
	1.61-1.90	117854	10.10	7	21.88	2.17	0.77	-0.14	0.91	0.43	
	1.91-2.38	118036	10.12	4	12.50	1.24	0.21	-0.03	0.24	0.53	
	2.39-3.54	115883	9.93	2	6.25	0.63	-0.46	0.04	-0.50	0.73	
	3.55-6.19	115970	9.94	5	15.63	1.57	0.45	-0.07	0.52	0.49	
	6.20-11.26	115651	9.91	1	3.13	0.32	-1.15	0.07	-1.23	1.02	
	11.27-25.24	115647	9.91	2	6.25	0.63	-0.46	0.04	-0.50	0.73	
	25.25-67.60	115630	9.91	4	12.50	1.26	0.23	-0.03	0.26	0.53	
	67.61-199.99	115609	9.91	1	3.13	0.32	-1.15	0.07	-1.23	1.02	
Na (ppm)	0.2200-0.5790	116685	10.00	0	0.00	0.00	NaN	0.11	NaN	NaN	-0.00046
	0.5791-0.6504	116721	10.01	1	3.13	0.31	-1.16	0.07	-1.24	1.02	
	0.6505-0.6959	116839	10.02	3	9.38	0.94	-0.07	0.01	-0.07	0.61	
	0.6960-0.7287	116664	10.00	3	9.38	0.94	-0.06	0.01	-0.07	0.61	
	0.7288-0.7844	116629	10.00	8	25.00	2.50	0.92	-0.18	1.10	0.41	
	0.7845-0.8366	116622	10.00	2	6.25	0.63	-0.47	0.04	-0.51	0.73	
	0.8367-0.8943	116676	10.00	3	9.38	0.94	-0.06	0.01	-0.07	0.61	
	0.8944-0.9611	116614	10.00	5	15.63	1.56	0.45	-0.06	0.51	0.49	
	0.9612-1.1210	116524	9.99	3	9.38	0.94	-0.06	0.01	-0.07	0.61	
	1.1211-4.1488	116464	9.98	4	12.50	1.25	0.22	-0.03	0.25	0.53	
Ni (ppb)	1.0001-5.3709	116644	10.00	2	6.25	0.62	-0.47	0.04	-0.51	0.73	-0.63794
	5.3710-8.8292	116646	10.00	4	12.50	1.25	0.22	-0.03	0.25	0.53	
	8.8293-10.4420	116644	10.00	3	9.38	0.94	-0.06	0.01	-0.07	0.61	
	10.4421-11.6711	116651	10.00	6	18.75	1.87	0.63	-0.10	0.73	0.45	
	11.6712-12.7538	116655	10.00	1	3.13	0.31	-1.16	0.07	-1.24	1.02	
	12.7539-13.9820	116648	10.00	2	6.25	0.62	-0.47	0.04	-0.51	0.73	
	13.9821-14.9556	116644	10.00	1	3.13	0.31	-1.16	0.07	-1.24	1.02	
	14.9557-15.9219	116646	10.00	1	3.13	0.31	-1.16	0.07	-1.24	1.02	
	15.9220-16.7251	116633	10.00	7	21.88	2.19	0.78	-0.14	0.92	0.43	
	16.7252-19.9999	116627	10.00	5	15.63	1.56	0.45	-0.06	0.51	0.49	
Pb (ppb)	1.00-8.76	116772	10.01	2	6.25	0.62	-0.47	0.04	-0.51	0.73	0.27793
	8.77-17.68	116678	10.00	5	15.63	1.56	0.45	-0.06	0.51	0.49	
	17.69-21.65	116889	10.02	0	0.00	0.00	NaN	0.11	NaN	NaN	
	21.66-24.56	117006	10.03	4	12.50	1.25	0.22	-0.03	0.25	0.53	
	24.57-27.30	116743	10.01	4	12.50	1.25	0.22	-0.03	0.25	0.53	
	27.31-30.38	116786	10.01	2	6.25	0.62	-0.47	0.04	-0.51	0.73	
	30.39-33.10	116634	10.00	1	3.13	0.31	-1.16	0.07	-1.24	1.02	
	33.11-36.51	116709	10.01	4	12.50	1.25	0.22	-0.03	0.25	0.53	
	36.52-39.37	116345	9.97	5	15.63	1.57	0.45	-0.06	0.51	0.49	
	39.38-49.99	115876	9.93	5	15.63	1.57	0.45	-0.07	0.52	0.49	
Si (ppm)	10.801-16.979	116655	10.00	3	9.38	0.94	-0.06	0.01	-0.07	0.61	0.00165
	16.980-18.317	116728	10.01	0	0.00	0.00	NaN	0.11	NaN	NaN	
	18.318-19.271	116675	10.00	2	6.25	0.62	-0.47	0.04	-0.51	0.73	
	19.272-20.521	116693	10.00	5	15.63	1.56	0.45	-0.06	0.51	0.49	

	20.522-21.914	116619	10.00	5	15.63	1.56	0.45	-0.06	0.51	0.49	
	21.915-23.443	116686	10.00	3	9.38	0.94	-0.06	0.01	-0.07	0.61	
	23.444-25.021	116607	10.00	1	3.13	0.31	-1.16	0.07	-1.24	1.02	
	25.022-27.559	116627	10.00	4	12.50	1.25	0.22	-0.03	0.25	0.53	
	27.560-31.012	116583	9.99	3	9.38	0.94	-0.06	0.01	-0.07	0.61	
	31.013-96.079	116565	9.99	6	18.75	1.88	0.63	-0.10	0.73	0.45	
Sr (ppb)	8.00-20.48	116702	10.00	3	9.38	0.94	-0.07	0.01	-0.07	0.61	-0.01602
	20.49-42.65	116644	10.00	6	18.75	1.87	0.63	-0.10	0.73	0.45	
	42.66-57.42	116749	10.01	1	3.13	0.31	-1.16	0.07	-1.24	1.02	
	57.43-66.48	116649	10.00	2	6.25	0.62	-0.47	0.04	-0.51	0.73	
	66.49-71.81	116821	10.02	2	6.25	0.62	-0.47	0.04	-0.51	0.73	
	71.82-76.94	116630	10.00	3	9.38	0.94	-0.06	0.01	-0.07	0.61	
	76.95-84.38	116686	10.00	7	21.88	2.19	0.78	-0.14	0.92	0.43	
	84.39-96.47	116540	9.99	4	12.50	1.25	0.22	-0.03	0.25	0.53	
	96.48-134.78	116509	9.99	4	12.50	1.25	0.22	-0.03	0.25	0.53	
	134.79-499.92	116508	9.99	0	0.00	0.00	NaN	0.11	NaN	NaN	
V (ppb)	10.000-10.001	116806	10.01	4	12.50	1.25	0.22	-0.03	0.25	0.53	0.53038
	10.002-10.320	116672	10.00	5	15.63	1.56	0.45	-0.06	0.51	0.49	
	10.321-10.744	116623	10.00	4	12.50	1.25	0.22	-0.03	0.25	0.53	
	10.745-11.616	116648	10.00	1	3.13	0.31	-1.16	0.07	-1.24	1.02	
	11.617-12.435	116656	10.00	4	12.50	1.25	0.22	-0.03	0.25	0.53	
	12.436-14.190	116633	10.00	4	12.50	1.25	0.22	-0.03	0.25	0.53	
	14.191-15.335	116625	10.00	1	3.13	0.31	-1.16	0.07	-1.24	1.02	
	15.336-17.900	116593	10.00	5	15.63	1.56	0.45	-0.06	0.51	0.49	
	17.901-20.623	116598	10.00	4	12.50	1.25	0.22	-0.03	0.25	0.53	
	20.624-99.985	116584	9.99	0	0.00	0.00	NaN	0.11	NaN	NaN	
W (ppb)	1.000-2.152	116858	10.02	1	3.13	0.31	-1.16	0.07	-1.24	1.02	-0.10819
	2.153-2.458	116646	10.00	2	6.25	0.62	-0.47	0.04	-0.51	0.73	
	2.459-2.683	116776	10.01	5	15.63	1.56	0.45	-0.06	0.51	0.49	
	2.684-2.988	116706	10.01	5	15.63	1.56	0.45	-0.06	0.51	0.49	
	2.989-3.363	116762	10.01	0	0.00	0.00	NaN	0.11	NaN	NaN	
	3.364-4.015	116577	9.99	5	15.63	1.56	0.45	-0.06	0.51	0.49	
	4.016-4.478	116788	10.01	4	12.50	1.25	0.22	-0.03	0.25	0.53	
	4.479-4.946	116606	10.00	6	18.75	1.88	0.63	-0.10	0.73	0.45	
	4.947-6.530	116366	9.98	4	12.50	1.25	0.23	-0.03	0.25	0.53	
	6.531-49.994	116353	9.98	0	0.00	0.00	NaN	0.11	NaN	NaN	
Zn (ppb)	1.00-3.28	117143	10.04	4	12.50	1.24	0.22	-0.03	0.25	0.53	0.06175
	3.29-4.34	117519	10.08	3	9.38	0.93	-0.07	0.01	-0.08	0.61	
	4.35-5.21	117200	10.05	1	3.13	0.31	-1.17	0.07	-1.24	1.02	
	5.22-6.13	116683	10.00	3	9.38	0.94	-0.06	0.01	-0.07	0.61	
	6.14-7.22	116931	10.02	3	9.38	0.94	-0.07	0.01	-0.07	0.61	
	7.23-8.81	116420	9.98	3	9.38	0.94	-0.06	0.01	-0.07	0.61	
	8.82-11.02	116562	9.99	2	6.25	0.63	-0.47	0.04	-0.51	0.73	
	11.03-13.62	116052	9.95	3	9.38	0.94	-0.06	0.01	-0.07	0.61	
	13.63-21.96	115998	9.94	4	12.50	1.26	0.23	-0.03	0.26	0.53	
	21.97-49.99	115930	9.94	6	18.75	1.89	0.63	-0.10	0.74	0.45	

Magnetic anomaly (nT)	-145--101	128137	10.99	3	9.38	0.85	-0.16	0.02	-0.18	0.61	-0.00657
	-100--92	121586	10.42	4	12.50	1.20	0.18	-0.02	0.21	0.53	
	-91--83	118890	10.19	6	18.75	1.84	0.61	-0.10	0.71	0.45	
	-82--76	131697	11.29	4	12.50	1.11	0.10	-0.01	0.12	0.53	
	-75--68	118478	10.16	3	9.38	0.92	-0.08	0.01	-0.09	0.61	
	-67--59	115975	9.94	4	12.50	1.26	0.23	-0.03	0.26	0.53	
	-58--49	115502	9.90	0	0.00	0.00	NaN	0.10	NaN	NaN	
	-48--32	110107	9.44	4	12.50	1.32	0.28	-0.03	0.32	0.53	
	-31--9	105926	9.08	2	6.25	0.69	-0.37	0.03	-0.40	0.73	
	-8-153	100140	8.59	2	6.25	0.73	-0.32	0.03	-0.34	0.73	
Distance from fault (m)	0-120	119087	10.21	0	0.00	0.00	NaN	0.11	NaN	NaN	0.00003
	123-256	118526	10.16	4	12.50	1.23	0.21	-0.03	0.23	0.53	
	258-408	118732	10.18	3	9.38	0.92	-0.08	0.01	-0.09	0.61	
	416-577	117138	10.04	7	21.88	2.18	0.78	-0.14	0.92	0.43	
	579-771	115748	9.92	5	15.63	1.57	0.45	-0.07	0.52	0.49	
	774-993	115764	9.92	2	6.25	0.63	-0.46	0.04	-0.50	0.73	
	994-1268	115499	9.90	3	9.38	0.95	-0.05	0.01	-0.06	0.61	
	1271-1632	115411	9.89	6	18.75	1.90	0.64	-0.10	0.74	0.45	
	1633-2292	115313	9.89	0	0.00	0.00	NaN	0.10	NaN	NaN	
	2294-6224	115220	9.88	2	6.25	0.63	-0.46	0.04	-0.50	0.73	
Lithology	Ogl	1064	0.09	0	0.00	0.00	NaN	0.00	NaN	NaN	-1.54617
	lgr	4841	0.42	0	0.00	0.00	NaN	0.00	NaN	NaN	-2.63001
	Di	14	0.00	0	0.00	0.00	NaN	0.00	NaN	NaN	-2.82522
	Hagr	245	0.02	0	0.00	0.00	NaN	0.00	NaN	NaN	-3.00918
	Hb	2281	0.20	2	6.25	31.96	3.46	-0.06	3.53	4.83	10.46756
	Oyb	1022	0.09	0	0.00	0.00	NaN	0.00	NaN	NaN	-1.30763
	Qr	49757	4.27	2	6.25	1.47	0.38	-0.02	0.40	0.55	8.51705
	Qd	533	0.05	0	0.00	0.00	NaN	0.00	NaN	NaN	-0.77791
	Kad	136	0.01	0	0.00	0.00	NaN	0.00	NaN	NaN	-2.43856
	Kbd	881	0.08	1	3.13	41.37	3.72	-0.03	3.75	3.69	12.86849
	Kfl	3	0.00	0	0.00	0.00	NaN	0.00	NaN	NaN	-2.66456
	Kgp	359	0.03	0	0.00	0.00	NaN	0.00	NaN	NaN	-0.74304
	Kh	262	0.02	0	0.00	0.00	NaN	0.00	NaN	NaN	0.00000
	Kj	792	0.07	0	0.00	0.00	NaN	0.00	NaN	NaN	-1.41765
	Kqp	520	0.04	0	0.00	0.00	NaN	0.00	NaN	NaN	-1.78021
	Ksgr	9862	0.85	0	0.00	0.00	NaN	0.01	NaN	NaN	-2.19213
	Jgr	19233	1.65	0	0.00	0.00	NaN	0.02	NaN	NaN	-3.80720
	Jgr	3466	0.30	0	0.00	0.00	NaN	0.00	NaN	NaN	-1.49119
	Jbs	584	0.05	0	0.00	0.00	NaN	0.00	NaN	NaN	-1.66856
	Jbc	3969	0.34	0	0.00	0.00	NaN	0.00	NaN	NaN	-1.74379
	TRn	20281	1.74	0	0.00	0.00	NaN	0.02	NaN	NaN	-0.32642
	TRn1	20837	1.79	0	0.00	0.00	NaN	0.02	NaN	NaN	-1.21220
	TRn2	12158	1.04	0	0.00	0.00	NaN	0.01	NaN	NaN	-0.83909
	TRn3	6944	0.60	0	0.00	0.00	NaN	0.01	NaN	NaN	-1.12328
	TRg	53754	4.61	0	0.00	0.00	NaN	0.05	NaN	NaN	-1.18890
	Ps	18150	1.56	0	0.00	0.00	NaN	0.02	NaN	NaN	-1.79743
	Ch	69942	6.00	0	0.00	0.00	NaN	0.06	NaN	NaN	-2.32484
	Oj	78322	6.71	1	3.13	0.47	-0.76	0.04	-0.80	-0.79	8.10235

	Omg	215666	18.49	8	25.00	1.35	0.30	-0.08	0.38	0.94	9.80276
	Odu	89243	7.65	4	12.50	1.63	0.49	-0.05	0.54	1.02	9.55816
	Od	6794	0.58	0	0.00	0.00	NaN	0.01	NaN	NaN	-1.58241
	CEw	129104	11.07	3	9.38	0.85	-0.17	0.02	-0.18	-0.30	8.72195
	CEp	112818	9.67	5	15.63	1.62	0.48	-0.07	0.55	1.13	8.86861
	CEm	58514	5.02	2	6.25	1.25	0.22	-0.01	0.23	0.32	7.71460
	CEj	17535	1.50	0	0.00	0.00	NaN	0.02	NaN	NaN	-3.25116
	PCEt	103955	8.91	2	6.25	0.70	-0.35	0.03	-0.38	-0.53	7.64571
	Jugr	52597	4.51	2	6.25	1.39	0.33	-0.02	0.34	0.47	7.53975

[a] Using the quantile classification method
[b] Likelihood ratio
[c] Constant value : - 19.07087

Table A1. Spatial relationship between mineral deposits and some related factors

9. References

Agterberg, F.P. & Bonham-Carter, G.F. (2005). Measuring performance of mineral-potential maps. *Natural Resources Research*, Vol. 14, No. 1, 1-17, ISSN 15207439

Agterberg, F.P. (1988). Application of recent developments of regression analysis in regional mineral resource evaluation, In: *Quantitative analysis of mineral and energy resources*, Chung, C.F.; Fabbri, G. & Sinding-Larsen, R. (Ed.), 1-28, D Reidel Publishing, ISBN 9027726353, Dordrecht

Agterberg, F.P.; Bonham-Carter, G.F. & Wright, D.F. (1990). Statistical pattern integration for mineral exploration, In: *Computer Applications in Resource Estimation Prediction and Assessment for Metals and Petroleum*, Gaal, G. & Merriam, D.F. (Ed.), 1-21, Pergamon Press, ISBN 01068667, Oxford

An, P. & Moon, W.M. (1993). An evidential reasoning structure for integrating geophysical, geological and remote sensing data, Proceedings of the International Geoscience and Remote Sensing Symposium (IGARSS), pp. 1359-1361, ISBN 0-7803-1240-6, August, 1993, Tokyo

An, P.; Moon, W.M. & Rencz, A.N. (1991). Application of fuzzy set theory to integrated mineral exploration. *Canadian Journal of Exploration Geophysics*, Vol. 27, No. 1, 1-11, ISSN

Atkinson, P.M. & Massari, R. (1998). Generalized linear modeling of susceptibility to landsliding in the central Apennines Italy. *Computers & Geosciences*, Vol. 24, No. 4, 373-385, ISSN 0098-3004

Behnia, P. (2007). Application of radial basis functional link networks to exploration for proterozoic mineral deposits in central Ira. *Natural Resources Research*, Vol. 16, No. 2, 147- 155, ISSN 15207439

Benomar, T.B.; Hu, G. & Bian, F. (2009). A predictive GIS model for potential mapping of copper, lead, and zinc in langping area, China. Geo-Spatial Information Science, Vol. 12, No. 4, 243-250, ISSN 10095020

Bonham-Carter, G.F. (1994). Geographic Information Systems for Geoscientists: Modeling with GIS, 398, Pergamon Press, ISBN 0 08 041867 8, Netherland

Bonham-Carter, G.F.; Agterberg, F.P. & Wright, D.F. (1988). Integration of geological datasets for gold exploration in Nova Scotia. *Photogrammetic Engineering and Remote Sensing*, Vol. 54, No. 11, 1585-1592, ISSN 00991112

Bonham-Carter, G.F.; Agterberg, F.P. & Wright, D.F. (1989). Weights of evidence modeling: A new approach to mapping mineral potential, In: *Statistical Applications in the Earth Sciences*, Agterberg, F.P. & Bonham-Carter. G.F. (Ed.), 171-183, Geological Survey of Canada 98, ISBN 0660135922, Canadian Government Publishing Centre

Brown, W.; Groves, D. & Gedeon, T. (2003). Use of Fuzzy Membership Input Layers to Combine Subjective Geological Knowledge and Empirical Data in a Neural Network Method for Mineral-Potential Mapping. *Natural Resources Research*, Vol. 12, No. 4, 183-200, ISSN 15207439

Brown, W.M.; Gedeon, T.D.; Groves, D.I. & Barnes, R.G. (2000). Artificial neural networks: a new method for mineral prospectively mapping. *Australian Journal of Earth Sciences*, Vol. 47, No. 4, 757-770, ISSN 08120099

Carranza, E.J.M. & Hale, M. (2000). Geologically constrained probabilistic mapping of gold potential, Baguio district, Philippines. *Natural Resources Research*, Vol. 9, No. 3, 237-253, ISSN 15207439

Carranza, E.J.M. (2004). Weights of evidence modeling of mineral potential: a case study using small number of prospects, Abra, Philippines. *Natural Resources Research*, Vol. 13, No. 3, 173-187, ISSN 15207439

Carranza, E.J.M.; Hale, M. & Faassen, C. (2008). Selection of coherent deposit-type locations and their application in data-driven mineral prospectivity mapping. *Ore geology reviews*, Vol. 33, No. 3-4, 536-558, ISSN 01691368

Carranza, E.J.M.; Woldai, T. & Chikambwe, E.M. (2005). Application of data-driven evidential belief functions to prospectivity mapping for aquamarine-bearing pegmatites, Lundazi District, Zambia. *Natural Resources Research*, Vol. 14, No. 1, 47-63, ISSN 15207439

Chi, K.H.; Lee, J.S.; Jin, M.S.; Chi, S.J. & Park, S.H. (2001). Construction of GIS based geological database of South Korea Area. *Korea Institute of Geoscience and Mineral Resources*, KR-01(T)-08, 210

Chung, C.F. & Agterberg, F.P. (1980). Regression models for estimating mineral resources from geological map data. *Mathematical Geology*, Vol. 12, No. 5, 473-488, ISSN 08828121

D'Ercole, C.; Groves, D.I. & Knox-Robinson, C.M. (2000). Using fuzzy logic in a Geographic Information System environment to enhance conceptually based prospectively analysis of Mississippi Valley-type mineralization. *Australian Journal of Earth Sciences*, Vol. 47, No. 5, 913-927, ISSN 08120099

De Quadros, T.F.P.; Koppe, J.C.; Strieder, A.J. & Costa, J.F.C.L. (2006). Mineral-potential mapping: A comparison of weights-of-evidence and fuzzy methods. *Natural Resources Research*, Vol. 15, No. 1, 49-65, ISSN 15207439

Eddy, B.G.; Bonham-Carter, G.F. & Jefferson, C.W. (1995). Mineral resource assessment of the Parry Islands, high Arctic, Canada: A GIS-base fuzzy logic model, Proceedings of Canadian Conference on GIS, CD ROM session C3, Paper 4, Ottawa

Garrett, J. (1994). Where and why artificial neural networks are applicable in civil engineering. *Journal of Computing in Civil Engineering*, Vol. 8, No. 2, 129-130, ISSN 0887-3801

Harris, D. & Pan, G. (1999). Mineral favorability mapping: A comparison of artificial neural networks, logistic regression, and discriminant analysis. *Natural Resources Research*, Vol. 8, No. 2, 93-109, ISSN 15207439

Harris, D.; Zurcher, L.; Stanley, M.; Marlow, J & Pan, G. (2003). A comparative analysis of favorability mappings by weights of evidence, probabilistic neural networks, discriminant analysis, and logistic regression. *Natural Resources Research*, Vol. 12, No. 4, 241-256, ISSN 15207439

Harris, J.R.; Lemkow, D.; Jefferson, C.; Wright, D. & Falck, H. (2008). Mineral potential modelling for the greater Nahanni ecosystem using GIS based analytical methods. Natural Resources Research, Vol. 17, No. 2, 51-78, ISSN 15207439

Hines, J.W. (1997). *Fuzzy and neural approaches in engineering*, Wiley, ISBN 978-0471192473, New York

Jianping, C.; Gongwen, W. & Changbo, H. (2005). Quantitative prediction and evaluation of mineral resources based on GIS: A case study in Sanjiang region, southwestern China. *Natural Resources Research*, Vol. 14, No. 4, 285-294, ISSN 15207439

Kim, J.C.; Koh, H.J.; Lee, S.R.; Lee, C.B.; Choi, S.J. & Park, K.H. (2001). Explanatory note the Gangreung-Sokcho Sheet. *Korean Institute of Geoscience and Mineral Resources*, KR-M 25-08 2001, 76

Kim, J.H.; Kee, W.S. & Seo, S.K. (1996). Geological structures of the Yeoryang-Imgye area, northern part of Mt. Taebaek Region, Korea. *The Journal of the Geological Society of Korea*, Vol. 32, No. 1, 1-15, ISSN 0435-4036

Knox-Robinson, C.M. (2000). Vectorial fuzzy logic: a novel technique for enhanced mineral prospectivity mapping, with reference to the orogenic gold mineralisation potential of the Kalgoorlie Terrane, Western Australia. *Australian Journal of Earth Sciences*, Vol. 47, No. 5, 929-941, ISSN 08120099

Koh, S.M.; Kim, S.Y.; Lee, D.J.; Kim, D.O.; Lee, H.Y.; Kim, Y.U.; Yoo, J.H.; Kim, Y.I.; Ryoo, C.R. & Song, M.S. (2003). Construction of the data-base and assessment of domestic mineral resources III (Area of 1:250,000 Seoul and Gangreung Geological Sheets). *Ministry of Commerce, Industry and Energy*, KR-2002-C-14-2003-R, 84

Koo, S.B.; Cho, J.D.; Lee, T.S.; Park, Y.S.; Lim, M.T.; Choi, J.H.; Sung, N.H.; Hwang, H.S. & Koh, I.S. (2001). Regional geophysical exploration. *Korean Institute of Geoscience and Mineral Resources*, KR-2000-R-11-2001-R, 70

Lee, C.H. & Park, H.I. (1996). Epithermal gold-silver mineralization and depositional environment carbonate-hosted replacement type Baegjeon Deposits, Korea. *Economic and Environmental Geology*, Vol. 29, No. 2, 105-117, ISSN 1225-7281

Lee, J.S.; Seo, H.J & Hwnag, I.H. (1998). Regional geochemical mapping of the Kangneung Sheet (1:250,000). *Korean Institute of Geoscience and Mineral Resources*, KR-98(C)-02, 147

Lee, S.; Ryu, J.H. & Kim, I.S. (2007). Landslide susceptibility analysis and its verification using likelihood ratio, logistic regression, and artificial neural network models: case study of Youngin, Korea. *Landslide*, Vol. 4, No. 4, 327-338, ISSN 1612510X

Leite, E.P. & Souza Filho, C.R. (2009). Artificial neural networks applied to mineral potential mapping for copper-gold mineralizations in the Carajas Mineral Province, Brazil. *Geophysical Prospecting*, Vol. 57, No. 3, 1049-1065, ISSN 00983004

Luo, X. & Dimitrakopoulos, R. (2003). Data-driven fuzzy analysis in quantitative mineral resource assessment. *Computers & Geosciences*, Vol. 29, No. 1, 3-13, ISSN 0098-3004

Moon, W.M. & So, C.S. (1995). Information representation and integration of multiple sets of spatial geoscience data, International Geoscience and Remote Sensing Symposium (IGARSS), pp. 2141-2144, ISBN 0-7803-2567-2, July, 1995, Firenze

Moon, W.M. (1990). Integration of geophysical and geological data using evidence theory function. *IEEE, Transactions on Geoscience and Remote Sensing*, Vol. 28, No. 4, 711-720, ISSN 0196-2892

Moon, W.M. (1993). On mathematical representation and integration of multiple spatial geoscience data sets. *Canadian Journal of Remote Sensing*, Vol. 19, No. 1, 63-67, ISSN 07038992

Nykänen, V. & Ojala, V.J. (2007). Spatial analysis techniques as successful mineral-potential mapping tools for orogenic gold deposits in the northern Fennoscandian shield, Finland. Natural Resources Research, Vol. 16, No. 2, 85-92, ISSN 15207439

Nykanen, V. & Raines, G.L. (2006). Quantitative analysis of scale of aeromagnetic data raises questions about geologic-map scale. *Natural Resources Research*, Vol. 15, No. 4, 213-222, ISSN 15207439

Nykanen, V. & Salmirinne, H. (2007). Prospectivity analysis of gold using regional geophysical and geochemical data from the Central Lapland Greenstone Belt, Finland, In: *Gold in the Central Lapland Greenstone Belt*, Ojala, V.J., (Ed.), 235–253, Geological Survey of Finland, Special Paper 44

Nykanen, V. (2008). Radial Basis Functional Link Nets Used as a Prospectivity Mapping Tool for Orogenic Gold Deposits Within the Central Lapland Greenstone Belt, Northern Fennoscandian Shield. *Natural Resources Research*, Vol. 17, No. 1, 29-47, ISSN 15207439

Oh, H.J. & Lee, S. (2008). Regional Probabilistic and Statistical Mineral Potential, Mapping of Gold – Silver Deposits Using GIS in the Gangreung Area, Korea. *Resource Geology*, Vol. 58, No. 2, 171 – 187, ISSN 13441698

Pan, G.C. (1996). Extended weights of evidence modeling for the pseudo-estimation of metalgrades. *Natural Resources Research*, Vol. 5, No. 1, 53-76, ISSN 15207439

Paola, J.D. & Schowengerdt, R.A. (1995). A review and analysis of backpropagation neural networks for classification of remotely-sensed multi-spectral imagery. *International Journal of Remote Sensing*, Vol. 16, No. 16, 3033-3058, ISSN 01431161

Park, H.I.; Chang, H.W. & Jin, M.S. (1988). K-Ar ages of mineral deposits in the Taebaek Mountain district. *The Journal of Korean Institute of Mining Geology*, Vol. 21, No. 1, 57-67, ISSN 0379-7546

Partington, G. (2010). Developing models using GIS to assess geological and economic risk: An example from VMS copper gold mineral exploration in Oman. *Ore Geology Reviews*, In Press, doi:10.1016/ j.oregeorev.2010.02.002

Porwal, A.; Carranza, E.J.M. & Hale, M. (2003). Artificial neural networks for mineral potential mapping: a case study from Aravalli Province, western India. *Natural Resources Research*, Vol. 12, No. 3, 155-177, ISSN 15207439

Porwal, A.; Carranza, E.J.M. & Hale, M. (2006). A hybrid fuzzy weights-of-evidence model for mineral potential mapping. *Natural Resources Research*, Vol. 15, No. 1, 1-14, ISSN 15207439

Raines, G.L. (1999). Evaluation of weights of evidence to predict epithermal-gold deposits in the Great Basin of the Western United States. *Natural Resources Research*, Vol. 8, No. 4, 257-276, ISSN 15207439

Raines, G.L.; Connors, K.A. & Chorlton, L.B. (2007). Porphyry copper deposit tract definition - A global analysis comparing geologic map scales. *Natural Resources Research*, Vol. 16, No. 2, 191-198, ISSN 15207439

Rencz, A.N.; Harris, J.R.; Watson, G.P. & Murphy, B. (1994). Data integration for mineral exploration in the Antigonish Highlands, Nova Scotia: Application of GIS and remote sensing. *Canadian Journal of Remote Sensing*, Vol. 20, No. 3, 257-267, ISSN 07038992

Rigol-Sanchez, J.P.; Chica-Olmo, M. & Abarca-Hernandez, F. (2003). Artificial neural networks as a tool for mineral potential mapping with GIS. *International Journal Remote Sensing*, Vol. 24, No. 5, 1151-1156, ISSN 01431161

Roy, R.; Cassard, D.; Cobbold, P.R.; Rossello, E.A.; Bailly, L. & Lips, A.L.W. (2006). Predictive mapping for copper-gold magmatic-hydrothermal systems in NW Argentina: Use of a regional-scale GIS, application of an expert-guided data-driven approach, and comparison with results from a continental-scale GIS. *Ore Geology Reviews*, Vol. 29, No. 3-4, 260-286, ISSN 01691368

Singer, D.A. & Kouda, R. (1996). Application of a feed forward neural network in the search for Kuroko deposits in the Hokuroku District, Japan. *Mathematical Geology*, Vol. 28, No. 8, 1017-1023, ISSN 08828121

Skabar, A. (2007). Modeling the spatial distribution of mineral deposits using neural networks. *Natural Resource Modeling*, Vol. 20, No. 3, 435-450, ISSN 1939-7445

Skabar, A.A. (2005). Mapping mineralization probabilities using multilayer perceptrons. *Natural Resources Research*, Vol. 14, No. 2, 109-123, ISSN 15207439

Tangestani, M.H. & Moore, F. (2001). Porphyry copper potential mapping using the weights-of-evidence modeling a GIS northern Shahr-e-Babak Iran. *Australian Journal of Earth Sciences*, Vol. 48, No. 5, 913-927, ISSN 08120099

Xu, S.; Cui, Z.K.; Yang, X.L. & Wang, G.J. (1992). A preliminary application of weights of evidence in gold exploration in Xionger mountain region. Henan province. *Mathematical Geology*, Vol. 24, No. 6, 663-674, ISSN 08828121

Zhou, W. (1999). Verification of the nonparametric characteristics of backpropagation neural networks for image classification. *IEEE Transactions on Geoscience and Remote Sensing*, Vol. 37, No. 2, 771-779, ISSN 0196-2892

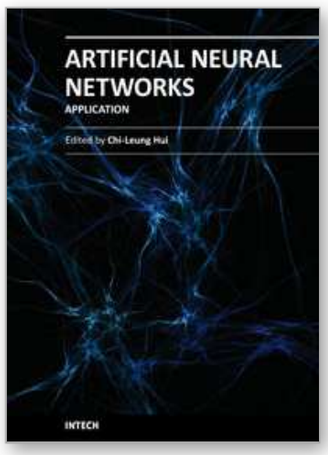

Artificial Neural Networks - Application

Edited by Dr. Chi Leung Patrick Hui

ISBN 978-953-307-188-6
Hard cover, 586 pages
Publisher InTech
Published online 11, April, 2011
Published in print edition April, 2011

This book covers 27 articles in the applications of artificial neural networks (ANN) in various disciplines which includes business, chemical technology, computing, engineering, environmental science, science and nanotechnology. They modeled the ANN with verification in different areas. They demonstrated that the ANN is very useful model and the ANN could be applied in problem solving and machine learning. This book is suitable for all professionals and scientists in understanding how ANN is applied in various areas.

InTech Europe
University Campus STeP Ri
Slavka Krautzeka 83/A
51000 Rijeka, Croatia
Phone: +385 (51) 770 447
Fax: +385 (51) 686 166
www.intechopen.com

InTech China
Unit 405, Office Block, Hotel Equatorial Shanghai
No.65, Yan An Road (West), Shanghai, 200040, China
中国上海市延安西路65号上海国际贵都大饭店办公楼405单元
Phone: +86-21-62489820
Fax: +86-21-62489821

IntechOpen